DPS-2: A Novel Dual MEK/ERK and PI3K/AKT Pathway Inhibitor with Powerful *Ex Vivo* and *In Vivo* Anticancer Properties

Maria Goulielmaki[*], Nikos Assimomytis[*], Jan Rozanc[†,1], Eleni Taki[*], Ioannis Christodoulou[*], Leonidas G. Alexopoulos[†,‡], Vassilis Zoumpourlis[*], Alexandros Pintzas[*] and Demetris Papahatjis[*]

[*]Institute of Biology Medicinal Chemistry and Biotechnology, National Hellenic Research Foundation, 116 36 Athens, Greece; [†]TEPA Lefkippos-Demokritos, Patriarchou Grigoriou & Neapoleos, 15343 Ag. Paraskevi, Attiki, Greece; [‡]School of Mechanical Engineering, National Technical University of Athens, Zografou 15780, Greece

Abstract

Development of novel bioactive compounds against KRAS and/or BRAF mutant colorectal cancer (CRC) is currently an urgent need in oncology. In addition, single or multitarget kinase inhibitors against MEK/ERK and PI3K/AKT pathways are of potential therapeutic advantage. A new compound based on the benzothiophene nucleus was synthesized, based on previous important outcomes on other pharmaceutical preparations, to be tested as potential anticancer agent. Treatments by 2-5 μM DPS-2 of several CRC and melanoma cell lines bearing either BRAF or KRAS mutations have shown a remarkable effect on cell viability in 2D and 3D cultures. More detailed analysis has shown that DPS-2 can kill cancer cells by apoptosis, reducing at the same time their autophagy properties. After testing activities of several signaling pathways, the compound was found to have a dual inhibition of two major proliferative/survival pathways, MEK/ERK and PI3K/AKT, in both CRC and melanoma, thus providing a mechanistic evidence for its potent anticancer activity. Antitumor activity of DPS-2 was further validated *in vivo*, as DPS-2 treatment of mouse xenografts of Colo-205 colorectal cancer cells remarkably reduced their tumor formation properties. Our findings suggest that DPS-2 has significant anti-KRAS/ anti-BRAF mutant CRC activity in preclinical models, potentially providing a novel treatment strategy for these difficult-to-treat tumors, which needs to be further exploited.

Translational Oncology (2019) 12, 932–950

Introduction

Colon cancer (CRC) is the fourth leading cause of cancer deaths worldwide. It results from the accumulation of multiple genetic and epigenetic alterations, leading to the transformation of colon epithelial cells into invasive adenocarcinomas [1]. Increasing knowledge of the major signaling pathways and molecular defects involved in colon carcinogenesis has led to the development of several novel target-based therapeutics, which have given encouraging results in patient outcome. Metastatic melanoma is also one of the most dangerous types of tumors. Within the most crucial pathways that become deregulated in these cancers belong the ERK/MAPK, JAK-STAT, PI3K/AKT/mTOR, and Wnt pathways [2–4]. The Ras/Raf/ MEK/ERK mitogen-activated protein kinase (ERK/MAPK) signaling pathway, involved in normal cell proliferation and survival, plays a critical role in colorectal and melanoma cancer progression since activating mutations of key genes like *RAS* and *BRAF* lead to

constitutive activation of the pathway, resulting in increased proliferation and tumor formation [5,6].

BRAF kinase, a key component of the ERK/MAPK signaling cascade, was found mutated in a variety of cancers [7]. Vemurafenib (PLX4032, Zelboraf) and dabrafenib are the most effective

BRAFV600E selective inhibitors and approved drugs for the treatment of BRAFV600E melanoma [8–10]. BRAFV600E mutant colorectal cancers are nonresponsive to its action due to, among other reasons, a feedback activation of EGFR [11–13]. Thus, combined treatment including BRAF and EGFR inhibition is shown to be of potent benefit for BRAF mutant colon cancer patients [14,15].

Other preclinical and/or therapeutic approaches regarding the ERK/MAPK signaling pathway include the use of MEK or even ERK inhibitors, which also offer the advantage of targeting this pathway in patients with either RAS or BRAF mutations [16–18]. Furthermore, combinations of BRAF and MEK inhibitors have come up with some encouraging results in clinical trials involving BRAF mutant colorectal cancer patients [19]. Combinations of MEK/ERK with PI3K/AKT pathway inhibitors have shown very promising preclinical and clinical efficiency. Upregulation of the PI3K/AKT pathway occurs in approximately 60% of CRC cases, which renders AKT a potential target for inhibition. Halilovic et al. observed increased antitumor activity with combined MEK and AKT inhibition in KRAS/PIK3CA-double-mutant HCT15. Mutant HCT15 tumor xenografts were treated with the MEK inhibitor PD0325901 and AKTi-1/2 alone or in combination [20]. Treatment with either agent alone had no significant effect on tumor growth; however, combined treatment abrogated the growth of tumor xenografts.

The existing therapies for the treatment of metastatic colorectal cancer include either antiangiogenetic agents, like bevacizumab and ramucirumab that target VEGF-A and VEGFR, respectively, or anti-EGFR antibodies, with a limitation of only K-RAS wild-type patients, like cetuximab or panitumumab, in combination with chemotherapy drugs like irinotecan, FOLFIRI, or FOLFOX [21–24]. Furthermore, since colorectal cancer is a highly heterogeneous disease with a set of different pathways involved in its development and progression, there are an increasing number of potent targets for therapy. Consequently, multikinase inhibitors, like the FDA-approved regorafenib and more under development, could be a therapeutic perspective for colorectal cancer and melanoma patients with a broader range of mutations.

Focusing on colorectal cancer, the absence of efficient drug treatments against KRAS- and BRAF- mutant tumors makes the development of new therapeutic agents an urgent need.

Benzothiophene compounds of the general formula, depicted in Figure 1, have been previously described as useful medications for the treatment of various medical indications associated with postmenopausal syndrome, uterine fibroid disease, endometriosis, and aortal smooth muscle cell proliferation (US005484798A). Virtually all of the known bioactive molecules may exhibit effects on biological targets other than those they were designed for. This property, termed

"drug repositioning," may result in repurposing of known bioactive substances, which refers to the process of finding new uses of existing compounds outside the scope of original indication.

This study was designed to test the hypothesis that DPS-2 (Figure 1), a newly synthesized small molecule, can act as a novel dual MEK-ERK and PI3K-AKT cell signaling pathway inhibitor coupled with potent anticancer properties in CRC and melanoma, both in cancer cell and in animal models. Notably, this agent has a significant apoptotic efficacy against mutant KRAS and BRAF cancer cells and tumors both *in vitro* and *in vivo*, for which specific efficient therapies are currently missing. The effect of the new compound DPS-2 on MEK/ERK and PI3K/AKT pathways known to be involved in colon cancer and melanoma progression is presented and discussed towards its potential further exploitation as an anticancer drug.

Materials and Methods

Experimental Procedures

^{1}H NMR spectra were recorded at 300 or 600 MHz on Varian 300 or 600 spectrometer. ^{13}C NMR spectra were recorded at 75 MHz on a Varian 300 spectrometer. ^{1}H NMR and ^{13}C NMR chemical shifts (δ) are reported in parts per million (ppm) relative to residual proton signals in $CDCl_3$ (δ = 7.26, 77.16 ppm), CD_3OD (δ = 4.87, 49.00 ppm), or DMSO-D6 (δ = 2.50, 39.43 ppm). Coupling constants (J) are reported in Hertz (Hz) and refer to apparent multiplicities. The following abbreviations are used for the multiplicities: singlet (s), doublet (d), triplet (t), quartet (q), multiplet (m), doublet of doublet (dd), doublet of triplet (dt), and broad (br). Melting points (m.p.) were determined on a Buchi 130 capillary melting point apparatus and are uncorrected. Mass spectra were recorded on a Thermo Fleet instrument by positive or negative electrospray ionization (ES^+ or ES^-). HRMS were recorded on a Thermo Velo instrument. Samples were infused in solution usually at 10-20 µl/min by means of a syringe pump. MeOH was used as solvent. TLC was carried out using Macherey-Nagel silica plates with a layer thickness of 0.25 mm SIL G-25 60 UV_{254}. Visualization was effected with ultraviolet light and phosphomolybdic acid reagent 10% in 95% ethanol. All solvents and reagents were obtained from commercial suppliers. Tetrahydrofurane was distilled from sodium/benzophenone ketyl.

2-(3-Methoxyphenylthio)-1-(4-methoxyphenyl)ethanone

Potassium hydroxide (0.662 g 10 mmol 85% purity) was added to a recently prepared solution of ethanol/water (10 ml EtOH/4.2 ml H_2O). To this solution, 3-mercaptoanisol (1) (1.402 g 10 mmol) was added, and the solution was cooled to 5°C. Then, a solution of 2-bromo-1-(4-methoxyphenyl)ethanone (2) (2.29 g 10 mmol) in ethyl acetate (6 ml) was added, and the reaction mixture was stirred at room temperature for about 18 hours. After this period, the reaction mixture was concentrated under reduced pressure, and the residue was dissolved in ethyl acetate (90 ml) and water (30 ml) The water phase was extracted with ethyl acetate (30 ml). The combined organic phases were washed with hydrochloric acid 5% (30 ml), water (30 ml), saturated solution of sodium bicarbonate (30 ml), water (30 ml), and saturated solution of sodium chloride (30 ml). After drying with anhydrous sodium sulfate, the solvent was removed in rotary evaporator. The remaining residue was recrystallized using ethyl acetate/petroleum ether to afford 2.3 g of the desired product. A
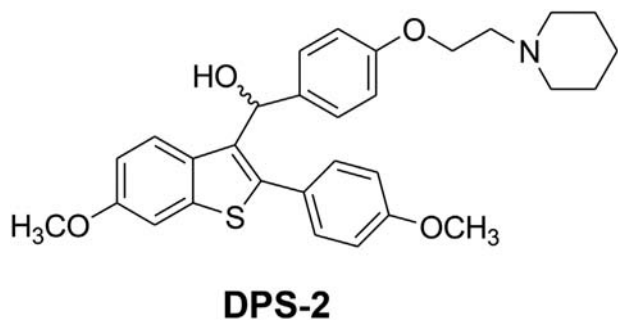
Figure 1. Chemical structure of DPS-2.

second crop of 0.15 g was obtained after a second recrystallization with ethyl acetate/hexane. Total yield 84%.

Rf (Et$_2$O/Pet. Ether 3:7) = 0.26 **m.p.** 51-53°C.

^{1}H NMR (600 MHz CDCl$_3$) δ 3.77 (s, 3H, -OCH_3), 3.87 (s, 3H, -OCH_3), 4.25 (s, 1H, -CH_2-), 6.72-6.77 (m, 1H, ArH), 6.92-6.98 (m, 4H, ArH),7.19 (t, 1H, ArH, J = 8.0 Hz), 7.93 (d, 2H, ArH, J = 8.9 Hz).

^{13}C NMR (75 MHz, CDCl$_3$) δ 40.85, 55.36, 55.62, 112.82, 113.95, 115.26, 122.13, 128.45, 129.94, 131.13, 136.53, 159.90, 163.91, 192.79.

6-Methoxy-2-(4-methoxyphenyl)benzo[b]thiophene

A round bottom flask with polyphosphoric acid (13.5 g) was heated at 85°C in oil bath under argon. To this viscous liquid was added at 85°C 2-(3-methoxyphenylthio)-1-(4-methoxyphenyl)etha-none (3) (2.2 g, 7.623 mmol) in small portions.The dark red–colored reaction mixture was stirred for 2 hours at 85°C under argon. Then, the reaction mixture was gradually cooled, and when the temperature was about 70°C, cold water and crushed ice were added slowly. After trituration with water, the dark red mixture solidified and remained in the freezer overnight. The beige solid was filtrated and added to a round-bottom flask with acetone (20 ml). The mixture was refluxed for 1 hour and then cooled in ice-bath. The off-white product was filtrated, and we obtained 1.26 g of the desired product. Yield 61%.

Rf (Et$_2$O/Pet. Ether 2:8) = 0.46.

^{1}H NMR (600 MHz DMSOD$_6$) δ 3.80 (s, 3H, -OCH_3), 3.82 (s, 3H, -OCH_3), 6.95-7.05 (m, 3H, ArH), 7.53 (d, 1H, ArH, J = 1.7 Hz), 7.61 (s, 1H, ArH,), 7.55-7.70 (m, 3H, ArH).

Methyl 4-(2-(piperidin-1-yl)ethoxy)benzoate (7)

A mixture of methyl 4 hydoxybenzoate (5) (0.68 g 4 mmol) anhydrous DMF (5 ml) and powdered anhydrous potassium carbonate (1.38 g,10 mmol) was heated to 100°C . Then, 1-(2-chloroethyl)piperidine hydrochloride (6) (0.99 g, 4.84 mol) was added in portion, over a period of 5 minutes. The reaction mixture was stirred at 100°C for about 3 hours. Then, the reaction was cooled at room temperature and diluted with 150 ml of ethyl acetate. The organic phase was washed with water (6×10 ml) and saturated solution of sodium chloride (1×10 ml), dried over anhydrous sodium sulfate, and evaporated *in vacuo*. The desired product was purified with flash column chromatography through a silica path using as eluent ethyl acetate/methanol 95:5. We received 0.99 g of a red-brown oil. Yield 84%.

Rf (MeOH/EtOAc 8:2) = 0.46.

^{1}H NMR (300 MHz MD$_3$OD) δ 1.4-1.8 (m, 6H, -CH_2-), 2.57 (m, 4H, -NCH_2), 2.81 (t, 2H, -CH_2N-, J = 5.6 Hz), 3.88(s, 3H, COOCH_3), 4.21 (t, 2H, -OCH_2-, J = 5.6 Hz) 6.95-7.05 (m, 2H, ArH), 7.90-8.00 (m, 2H, ArH).

^{13}C NMR (75 MHz, MD$_3$OD) δ 25.00, 26.47, 52.35, 55.91, 58.76, 66.69, 115.32, 123.70, 132.58, 164.13, 168.33.

MS-ESI *m/z* 264.20 [M + H]$^+$.

4-(2-(Piperidin-1-yl)ethoxy)benzoic acid hydrochloride

Methyl 4-(2-(piperidin-1-yl)ethoxy)benzoate (7) (0.99 g 3.75 mmol) was dissolved in MeOH (4 ml). Then 5 N solution of sodium hydroxide (1.8 ml) was added, and the reaction was allowed to stir at room temperature for 24 hours. The mixture was evaporated and the residue diluted with water (30 ml). The resulting solution

was cooled to 5°C and acidified with 6 N hydrochloric acid. The mixture was filtrated and the crystals were washed with cold MeOH. We received 0.95 g of a light beige product and the yield was 89%.

Rf (MeOH/EtOAc 8:2) = 0.34.

^{1}H NMR (300 MHz MD$_3$OD) δ 1.4-2.15 (m, 6H, -CH_2-), 3.12 (td, 2H, -CH_2N-, J = 13.0, 8.2 Hz), .3.25-3.4 (m, 4H, -NCH_2-), 4.49 (t, 2H, -OCH_2-, J = 4.8 Hz) 7.00-7.20 (m, 2H, ArH), 7.95-8.15 (m, 2H, ArH).

^{13}C NMR (75 MHz, MD$_3$OD) δ 22.53, 24.06, 54.92, 57.02, 63.34, 115.42, 125.34, 132.93, 162.81, 169.39.

MS-ESI *m/z* 250.22 [M + H]$^+$ (calc. For C$_{14}$H$_{19}$NO$_3$).

(4-(2-(Piperidin-1-yl)ethoxy)phenyl)(6-methoxy-2-(4-methoxy-phenyl)benzo[b] thiophen-3-yl)methanone hydrochloride

To a round-bottom flask were added 4-(2-(piperidin-1-yl)ethoxy) benzoic acid hydrochloride (8) (0.81 g, 2.825 mmol), chlorobenzene (9 ml), thionyl chloride (0.15 ml,) and DMF (0.2 ml). The reaction mixture was stirred for 2 hours at 75°C-80°C under argon. Excess of thionyl chloride and chlorobenzene was removed by vacuum distillation. Vacuum distillation was repeated with fresh chloroben-zene (5 ml) in order to remove any remaining quantity of thionyl chloride. Then, dry methylene chloride (15 ml) was added to the residue. To the corresponding solution were added 6-methoxy-2-(4-methoxyphenyl)benzo[b]thiophene (4) (0.75 g, 2.78 mmol) and aluminum trichloride (2.3 g 24 mmol). The mixture was stirred at 27°C-29°C for 2 hours. The reaction was quenched at 5°C-10°C by adding THF (10 ml) hydrochloric acid 20%(3 ml) and water (10 ml). The aqueous phase was removed and was extracted with methylene chloride (3×20 ml). The combined organic phases were extracted with water (15 ml) dried over anhydrous sodium sulfate and evaporated under reduced pressure. The remaining oil was purified with flash column chromatography using CHCl$_3$/MeOH 96:4 as eluent in order to furnish 0.91 g of the desired product as a yellow oil. Yield 61%.

Rf (CHCl$_3$/MeOH 9:1) = 0.56.

^{1}H NMR (300 MHz CDCl$_3$) δ 1.45-1.6 (m, 2H, -CH_2-),1.65-1.85 (m, 4H, -CH_2-), 2.6-2.8 (m, 4H, -NCH_2-), 2.94 (t, 2H, -CH_2N-, J = 5.4 Hz), 3.73 (s, 3H, -OCH_3,), 3.86 (s, 3H, -OCH_3), 4.23 (t, 2H, -OCH_2-, J = 5.4 Hz), 6.74 (d, 4H, ArH, J = 8.6 Hz,), 6.94 (dd, 1H, ArH, J = 8.9, 2.4 Hz), 7.28-7.37 (m, 3H, ArH), 7.50 (d, 1H, ArH, J = 8.9 Hz), 7.70-7.80 (m, 2H, ArH).

^{13}C NMR (75 MHz, CDCl$_3$) δ 23.33, 24.75, 54.75, 57.14, 65.02, 104.59, 114.18, 114.29, 114.090, 126.05, 130.35, 130,53, 130,87, 132.44, 134.01, 140.15, 142.72, 157.75, 159.84, 162.36, 193.17.

MS-ESI *m/z* 502.20 [M + H]$^+$ (calc. For C$_{30}$H$_{31}$NO$_4$S), 524.18 [M + Na]$^+$.

(4-(2-(Piperidin-1-yl)ethoxy)phenyl)(6-methoxy-2-(4-methoxy-phenyl)benzo[b] thiophen-3-yl)methanol (DPS-2)

(4-(2-(piperidin-1-yl)ethoxy)phenyl)(6-methoxy-2-(4-methoxy-phenyl)benzo[b] thiophen-3-yl)methanone hydrochloride (9) (0.120 g 0.2088 mmol) was dissolved in THF (1.2 ml), and the corresponding solution was cooled at 0°C . Then, lithium aluminum hydride was added (0.019 g 0.5 mmol), and the reaction mixture was stirred at 0°C for 45 minutes under argon. After the completion of the reaction (as monitored by tlc), THF (3 ml), THF/H$_2$O (4 ml), and H$_2$O (4 ml) were added. The product was extracted with methylene chloride (2×30 ml), and the organic phase was washed

with water (10 ml) and saturated solution of sodium chloride (10 ml), dried over anhydrous sodium sulfate, and concentrated *in vacuo*. The residue was purified with flash column chromatography by using $CHCl_3$/MeOH (97:3) as eluent. We obtained 0.1 g of a light yellow oil which solidified after staying in the freezer. Yield 89%.

Rf ($CHCl_3$/MeOH 9:1) = 0.40.

^{1}H NMR (300 MHz $CDCl_3$) δ 1.35-1.5 (m, 2H, -CH_2-),1.55-1.65 (m, 4H, -CH_2-), 2.4-2.55 (m, 4H, -NCH_2-), 2.74 (t, 2H, -CH_2N-, J = 6 Hz), 3.82 (s, 6H, -OCH_3), 4.23 (t, *J* = 6 Hz, 2H, -OCH_2), 6.15 (s, 1H, -HOCH), 6.75-6.85 (m,3H, ArH),), 6.87-6.97 (m, 2H, ArH), 7.27 (s, 1H, ArH), 7.30 (d, 2H, ArH, J = 8.4 Hz), 7.37-7.47 (m, 2H, ArH), 7.59(d, 1H, ArH, J = 8.4 Hz).

^{13}C NMR (75 MHz, $CDCl_3$) δ 24.01, 25.64, 54.93, 57.79, 65.64, 69.46, 69.52, 104.67, 113.80, 114.11, 114.33, 125.48, 126.19, 127.44, 130.83, 132.01, 132.52, 134.83, 138.95, 140.72, 157.09, 157.81, 159.71.

MS-ESI *m/z* 504.41 [M + H]$^+$.

HRMS *m/z* 504.2199 [M + H]$^+$ (calc. For $C_{30}H_{34}NO_4S$ 504.2203).

Cell Lines and Treatments

RKO, HT29, Colo-205, DLD-1, and HCT116 human colon adenocarcinoma; Caco-2 colon adenoma; NIH3T3 mouse embryo fibroblast; and HepG2 human hepatocellular carcinoma cell lines were obtained from American Type Culture Collection. All cell lines used in this study were grown in DMEM supplemented with 10% fetal bovine serum (FBS), antibiotics, and amino acids (all from Invitrogen). PLX4720 (#S1152, SELLECKCHEM) was used as a control for the inhibition of the BRAF/MEK/ERK signaling pathway. Human recombinant SuperKiller cc-TRAIL (ALX-522-020, Alexis) was used as a control of apoptotic cell death.

Four melanoma cell lines with BRAF mutation (WM35, WM3248, A375, SK-MEL19) and one NRAS mutated (WM3060) cell line were cultured in RPMI 1640 medium supplemented with 10% FBS. Cell lines were seeded on 96-well plates (10,000 cells/well). The following day, cells were treated in triplicates with increasing concentrations (1 μM, 2 μM, 5 μM, and 10 μM) of DPS-2. Cell viability was assessed after 24 and 72 hours using resazurin reduction assay.

WJ-MSCs Isolation and Characterization

For *in vitro* assays, human mesenchymal stem cells were isolated from Wharton's jelly (matrix) of the human fetal umbilical cord derived from full-term pregnancies (WJ-MSCs), as described in Christodoulou et al. [25]. The cells were characterized for the expression of surface markers by flow cytometry and were positive for CD29 (b1-integrin), CD44 (H-CAM), CD73 (ECTO-5′ nuclease/ SH3), CD90 (THY-1), and CD105 (endoglin/ SH2) and negative for CD14 (LeuM3/ MY4), CD34 (HPCA1/ gp105-120), and CD45 (LCA) [25].

WJ-MSCs up to seventh passage (<22 population doublings) were used for the experiments. At these culture points, cells maintained a stable MSC immunophenotypic profile as described above, and mean population doubling time (PDT) was 32+/– hours. Cells were propagated in culture as described before [25]. Briefly, cells were plated in flasks of 75 cm^2 and cultured in growth medium (GM), which consisted of DMEM/F12 (with 3.5 g/L glucose, ultragluta-mine I and Na pyruvate; Lonza) supplemented with 10% FBS, 15 mM HEPES, 1× nonessential amino acids, 1% penicillin/ streptomycin, and 2 mM Fungizone (all from Invitrogen). The cells

were maintained in a humidified atmosphere with 5% CO^2 in air at 37°C with total medium changes every 3-4 days until 70%-80% confluence. Subculturing (passages) was performed by trypsinization using 0.05% trypsin-EDTA solution (Invitrogen), and the cells were resuspended at a density of 4000 cells/cm^2 in flasks of 75 cm^2. Frozen stocks of 0.5-2 million cells were also kept in cryovials (Nunc) in 2 ml of 10% DMSO and FBS, which were stored in liquid N_2.

Western Blotting

Whole cell lysates were prepared using lysis buffer. Extracts were resolved on SDS-PAGE and transferred to a nitrocellulose membrane (Whatman, Scheicher & Schuell, Dassel, Germany). Membranes were incubated with specific antibodies in an indicated dilution overnight at 4°C, washed, and incubated with the appropriate secondary antibody for 1 hour at room temperature. Primary antibodies were used against pAKT (ser473) #9271, pAKT (thr308) #9275, p-SAPK/JNK (Thr183/Tyr185) #9251, pS6R (s235/236) #2211, pMEK (s217/221) #9121, Caspase-3 #9662, and cleaved caspase-3 (Asp175) #9661 from Cell Signaling (Danvers, MA, USA); SQSTM1/p62 (sc-28,359), PARP-1 (sc-7150), pERK (sc-7383), p-p38 (sc-7973), Actin (sc-8432), and a-Tubulin (sc-8035) were purchased from Santa Cruz (Biotechnology, Inc., 2145 Delaware Avenue, Santa Cruz, CA 95060 USA). Purified mouse Anti-RIP (610458) was obtained from BD Transduction Laboratories and RIPK3 (NBP2-24588) from Novus Biologicals. Secondary andibodies were goat anti-mouse (sc-2005, Santa Cruz) and goat anti-rabbit (#111-035-003, Jackson). Antibody signal was obtained with the enhanced chemiluminescence plus Western blotting detection system (Amersham Biosciences, Uppsala, Sweden) after exposure to Kodak Super RX film. Values were measured using the Image Studio Lite 4.0 software (LI-COR Biosciences), and protein levels were normalized against tubulin or actin. Experiments were independently repeated at least two times.

Two-Dimensional Culture

For the 2D culture experiments, cells (5000 cells/well) were grown on coverslips in 24-well plates in medium at 37°C. Photographs of the 2D cultures were taken under light and confocal microscope (Leica 626 TCS SPE confocal laser scanning microscope after the appropriate staining). LAS AF software was used for image 627 acquisition (Leica Lasertechnik, Heidelberg, Germany). Cells were fixed with 4% paraformaldehyde, washed with PBS, and perme-abilized with 0.25% Triton. Cell cytoskeleton was stained with phalloidin (Alexa Fluor 546, A22283, Life Technologies). Nuclei were stained with Hoechst No. 33342 (Sigma, B2261) for apoptosis detection; cleaved caspase-3 marker of apoptosis was detected by cleaved caspase-3 antibody. Secondary green fluorescent anti-rabbit antibody (Alexa Fluor 488, #A11008, Invitrogen) was used against primary anti–cleaved caspase-3 antibody.

Three-Dimensional Culture

For 3D culture experiments, cells were grown in 24-well plates on 30% Matrigel (BD Bioscience) that was allowed to set for 15 minutes at 37°C in order to form a gel of 1-mm thickness. The bottom layer was then covered with $2 × 10^3$ cells mixed 1:1 with 30% Matrigel in a total volume of 600 μl. Growth medium containing 2% Matrigel was replaced every 2 days, and the cells were left to grow for 12-14 days to allow development of extensive tubule network, after which treatment with inhibitor was applied for indicated incubation
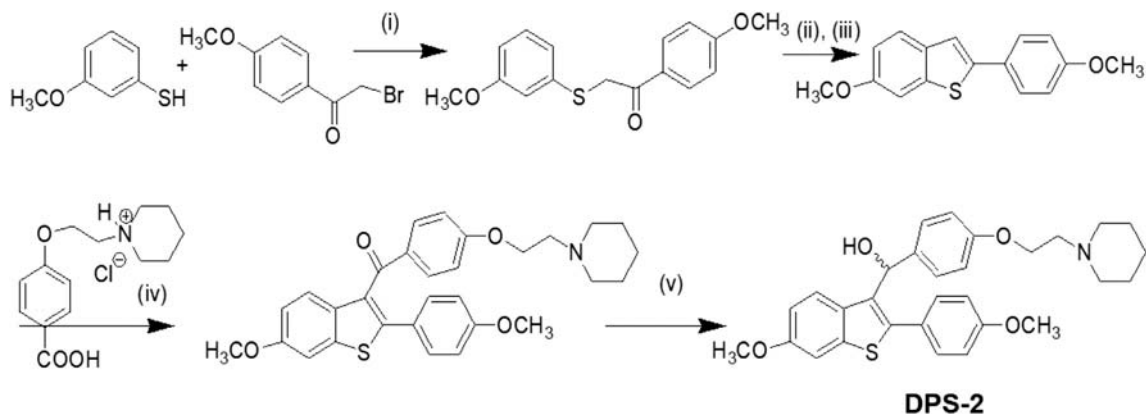
Figure 2. Chemical synthesis of DPS-2. (i) KOH, EtOH/H$_2$O/EtOAc, RT, 18 hours, 85%, (ii) PPA, 85°C , 2 hours, (iii) Acetone, reflux, 1 hour, 61% (in two steps), (iv) SOCl$_2$ / AlCl$_3$, C$_6$H$_5$Cl, 75°C , 2 hours, DCM, 1 hour RT, 62%, (v) LAH, THF, 0°C , 45 min, 94%.

times. Photographs of the 3D cultures were taken using a Nikon Eclipse T-200 inverted phase-contrast microscope equipped with an Olympus digital camera. The nuclei were stained with Hoechst No. 33342; the cleaved caspase-3 was detected with cleaved caspase-3–specific antibody.

Cell Viability Assays

SRB Assay. For growth studies on colon cancer cell lines, the sulforhodamine B (SRB, SIGMA) assay was used. Firstly, tumor cells were seeded into 96-well microtiter plates and were allowed to attach overnight. Thereafter, the cell number in treated *versus* control wells was estimated after treatment with 10% trichloroacetic acid and staining with 0.4% SRB in 1% acetic acid. The percentage of viable cell was plotted each time. SD was used for error bar generation.

MTS Viability/Cytotoxicity Assay. Cell viability of NIH3T3, HepG2 cells, and WJ-MSCs was determined colorimetrically in a 96-well plate assay using the tetrazolium compound MTS, which is bioreduced by cells into a colored formazan product that is soluble in tissue culture medium [26]. This conversion is presumably accomplished by NADPH or NADH produced by dehydrogenase enzymes in metabolically active (viable) cells.

The MTS (CellTiter 96 AQueousOne, Promega, USA) assay was performed following the manufacturer's recommendations. Briefly, NIH3T3, HEPG2 cells, and WJ-MSCs were plated into 96-well microtiter plates at a concentration of 2.5×10^3, 5×10^3 cells and 3.5×10^3/200 µl culture medium/well (37°C/5% CO^2). After 24-48 hours, the medium was removed, and the cells were treated with up to eight different concentrations of DPS-2, diluted in 200 µl growth medium per well. The control sample was incubated with adding only growth medium. The 0.2% DMSO (Sigma) diluted in DMEM was used as a negative control. Cells were then incubated for another 48 hours. After the incubation period, the chemical solutions were removed from all the plates, and the cells were washed with 150 µl/well of prewarmed PBS. Next, 100 µl/well of culture medium (without phenol red, L-glutamine, HEPES) and 20 ml of CellTiter 96 AQueous One Solution Reagent (Promega) were added to each well. The CellTiter 96 AQueous One Solution Cell Proliferation Assay is a colorimetric method for determining the number of viable cells in proliferation assays or cytotoxicity. In blank wells, PBS was added. The cells were incubated for 3 hours. At the end of each hour, the absorbance was measured at 490 nm (with 650 nm as a reference

wavelength) in a microplate reader (monochromator) [Monochromator Microplate Reader safire2 TECAN AUSTRIA GMBH/ Measurement parameter Editor Magellan (version 6)].

Statistical Analysis

All data are presented as the mean ± standard error. Results were analyzed in Microsoft Excel 2011, and mean values and standard deviations were estimated. Calculation of IC$_{50}$ values was performed using Graphpad Prism 6.0.

Phosphoprotein ELISA Measurements

For phosphoproteomic analysis, cells were seeded on 96-well plates at 20,000 cells/well. The following day, increasing concentrations of DPS-2 (1 µM, 2 µM, 5 µM, and 10 µM) were added to the cells in triplicates for 24 hours. After incubation, the medium was removed and cells were lysed directly in the wells with Protavio lysis buffer mix. Triplicates of the cell lysates were pulled together and normalized according to total protein concentration of the samples. Bead-based Luminex ELISA assays were used in a multiplex format to quantify the activity of phosphoproteins.

In Vivo Studies

The procedures in animals were performed in accordance with local animal ethics committees. A total of 2×10^6 Colo-205 cells diluted in PBS were injected subcutaneously in both left and right flanks of athymic mice. Tumors were allowed to grow for 8 days before inhibitor treatment was initiated. The mice were separated into three groups: untreated (four mice), DMSO treated (three mice), and inhibitor treated (five mice). The group of untreated mice was not given anything. DMSO mice were injected daily with 100 µl of 5% DMSO diluted in water. Inhibitor-treated mice were injected daily with 100 µl of the inhibitor in a final concentration of 0.6 µg/µl diluted in 5% DMSO. All injections of DMSO and inhibitor were performed intratumorally. Tumor sizes were measured with calipers every 3-4 days for a total period of 19 days after the injection of cancer cells. Tumor volume was calculated by the formula (V = length × width × depth), and comparative graphs were created. SD was used for error bar generation between all tumors of the same group of animals. Statistical analysis of the data was performed using two-way ANOVA, repeated measures test in Graphpad Priam 6.0. Mice were sacrificed only due to tumor burden.

Results

Chemistry

Synthesis of DPS-2. The key intermediate 6-methoxy-2-2(4-methoxyphenyl)-benzo[*b*]thiophene was prepared by the cyclization rearrangement produced by polyphosphoric acid (PPA) as described in the literature by Jones [27] and is depicted in Figure 2. The intermediate ether side chain methyl 4-(2-(piperidin-1-yl)ethoxy) benzoic acid hydrochloride was prepared by alkylation of methyl *p*-hydroxybenzoate with 1-(2-chloroethyl) piperidine hydrochloride by
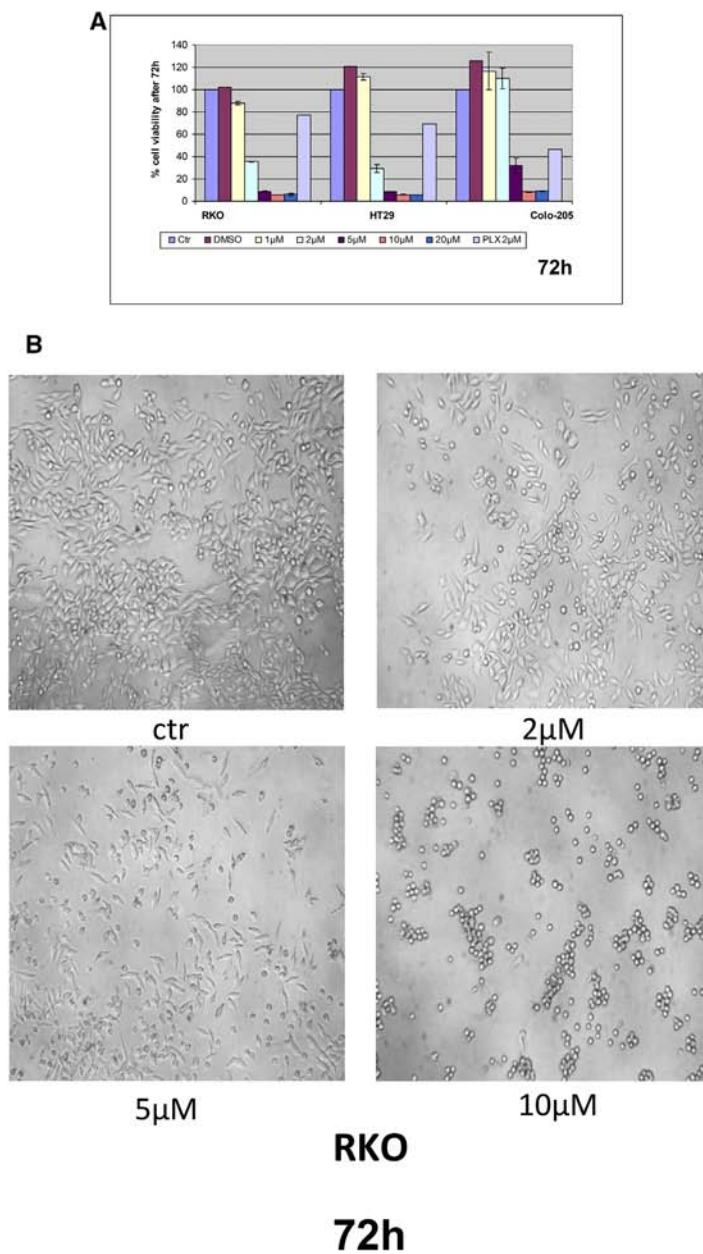
Figure 3. DPS-2 dramatically reduces cell viability of colon and melanoma cancer cell lines, while it affects cell viability of NIH3T3 and HepG2 cells in higher concentrations and shows very low toxicity in WJ-MSCs. (A) Cell Viability in RKO, HT29, and Colo-205 cell lines was measured using the SRB assay after 72-hour treatment with increasing concentrations of DPS-2 inhibitor. PLX4720 inhibitor was used as a positive control for cell viability reduction. (B) Light microscope images of 2D culture in RKO cell line after treatment with 2 μM, 5 μM, and 10 μM of DPS-2 inhibitor for 72 hours. (C) Cell Viability in Caco-2, HCT116, and DLD-1 cell lines was measured, using the SRB assay, after 72-hour treatment with increasing concentrations of DPS-2 inhibitor. Data are representative for two independent experiments, each of which was performed in duplicates. SD was used for error bar generation. (D) The effect of different concentrations (0-10 μM) of DPS-2 in five melanoma cell lines treated for 24 and 72 hours. All data are presented as the mean ± SD. (E) Percentage of cytotoxicity in WJ-MSCs cells after 48 hours of incubation with various concentrations of DPS-2 and respective survival curves (y = % viability, x = concentration μM). Cell viability was assessed using the MTS assay. Data are presented as mean of cell survival compared with negative control (cell survival assumed 100%). (F) Cell viability in NIH3T3 cell line was measured after 48-hour treatment with increasing concentrations of DPS-2 inhibitor. (G) Cell viability in HepG2 cell line was measured after 48-hour treatment with increasing concentrations of DPS-2 inhibitor. Cell viability was assessed using the MTS assay. Data are presented as mean of cell survival compared with negative control (cell survival assumed 100%). The 0.2% DMSO diluted in DMEM was used as a negative control for cell viability reduction. IC_{50} values are given for each graph. Experiments were performed in triplicates. SD was used for error bar generation.

Figure 3. (*continued*.)

Effect of DPS-2 on cell viability of colon cancer and melanoma cell lines

We initially examined the effect of DPS-2 on cell viability of colon cancer cell lines, bearing a different set of mutations, in order to have a primary assessment of the compound's efficacy as an antiproliferative agent in colon tumors. Towards this direction, DPS-2 managed to reduce
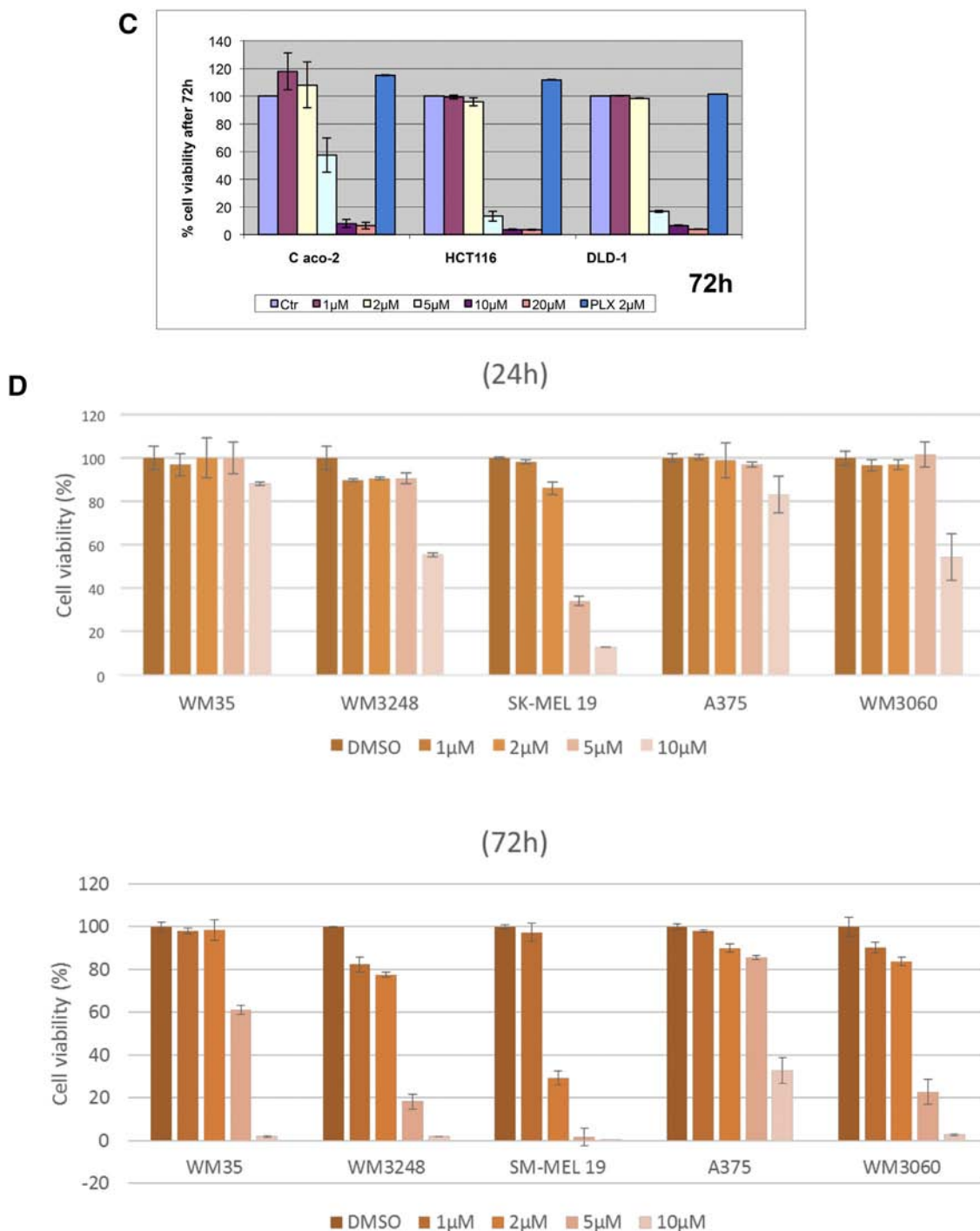
means of powdered anhydrous potassium carbonate followed by base hydrolysis. Friedel-Crafts aroylation of 6-methoxy-2-2(4-methoxyphenyl)-benzo[*b*]thiophene with methyl 4-(2-(piperidin-1-yl)ethoxy)benzoic acid chloride and LAH reduction of the corresponding benzo[*b*]thien-3-yl ketone provided the desired DPS-2 (Figure 2).

cell viability by more than 70% in all tested colon cancer cell lines, RKO, HT29, Colo-205, HCT116, and DLD-1, in concentration equal to or higher than 5 μM after 72-hour treatment (Figure 3, *A* and *C*). Caco-2, an intermediate adenoma cell line, was more resistant to the treatment with 5 μM of DPS-2, with an average reduction of 40% in cell viability (Figure 3C). All tested cell lines showed resistance to the action of the compound when treated with concentrations lower than 2 μM for 72 hours (Figure 3, *A-C*). PLX4720, a BRAFV600E selective inhibitor, was used a control for the reduction of cell viability in RKO, HT29, and Colo-205 cell lines, bearing the BRAFV600E mutation.

We then investigated the effect of DPS-2 on cell viability in five different melanoma cell lines (Figure 3D). All the cells had decreased survival rates;

E

DP-BRAF 2 in WJ-MSCs
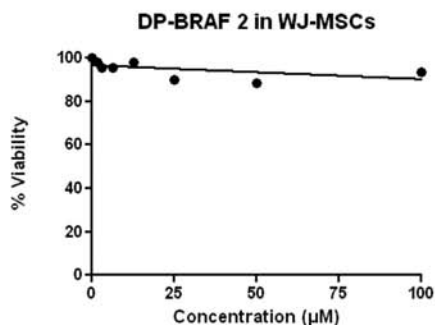
Toxicity	Concentration (µM)	100,00	50,00	25,00	12,50	6,25	3,13	1,56	0
	% Viability	93,56	88,25	90	98,2	95,56	95,74	97,9	100

F

NIH3T3

G

HepG2
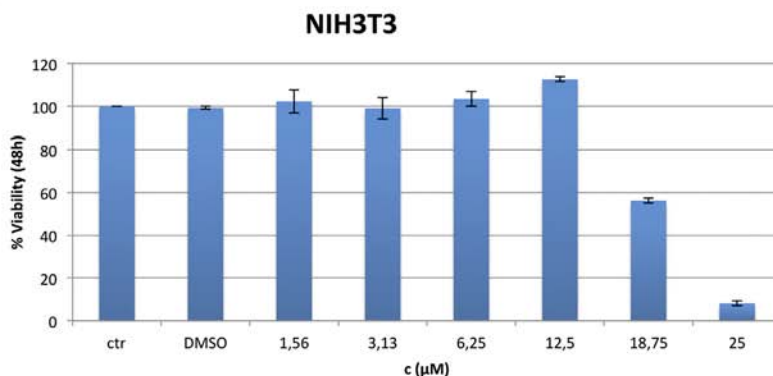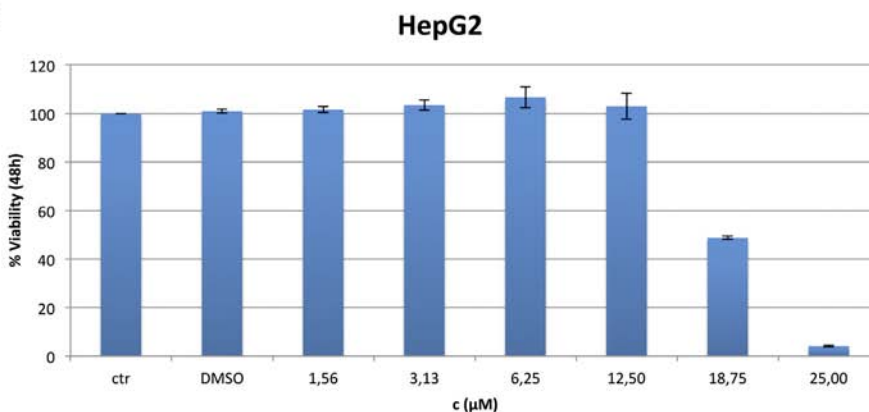
Figure 3. (*continued.*)

however, there was a difference in sensitivity to DPS-2 induced effects. The more sensitive V600E BRAF mutated cell lines SK-MEL19 and WM3248 exhibited the greatest overall decrease in viability with IC50 < 5 µM, whereas the more resistant cell lines (WM35 and A375) had less of a response to increasing concentrations of DPS-2. Moreover, the NRAS Q61K mutated WM3060 cell line showed significant sensitivity to DPS-2 with IC50 < 5 µM (Figure 3D). The five cell lines with different mutations and survival rates were further used for phosphoprotein measurements presented in Figure 4C. Since DPS-2 presents a dramatic effect on cell viability of tumor cells, the potential cell toxicity was tested in appropriate models. Thus, the *in vitro* response of WJ-MSCs to eight concentrations of DPS-2 and of NIH3T3 and HepG2 cells to seven concentrations of DPS-2 was tested. The two latter cell lines share similar characteristics with those proposed by the Interagency Coordinating Committee on the Validation of Alternative Methods (ICCVAM) for toxicity studies [28]. Human umbilical cord stem cells, WJ-MSCs, retained their viability even when they were treated with the highest concentrations of the compounds (Figure 3, E-G). NIH3T3 and HepG2 were also resistant, with IC50 values of 18.75 µM and 18.67 µM, respectively. This indicates a selective effect of this agent towards tumor cell lines while leaving unaffected normal cells.
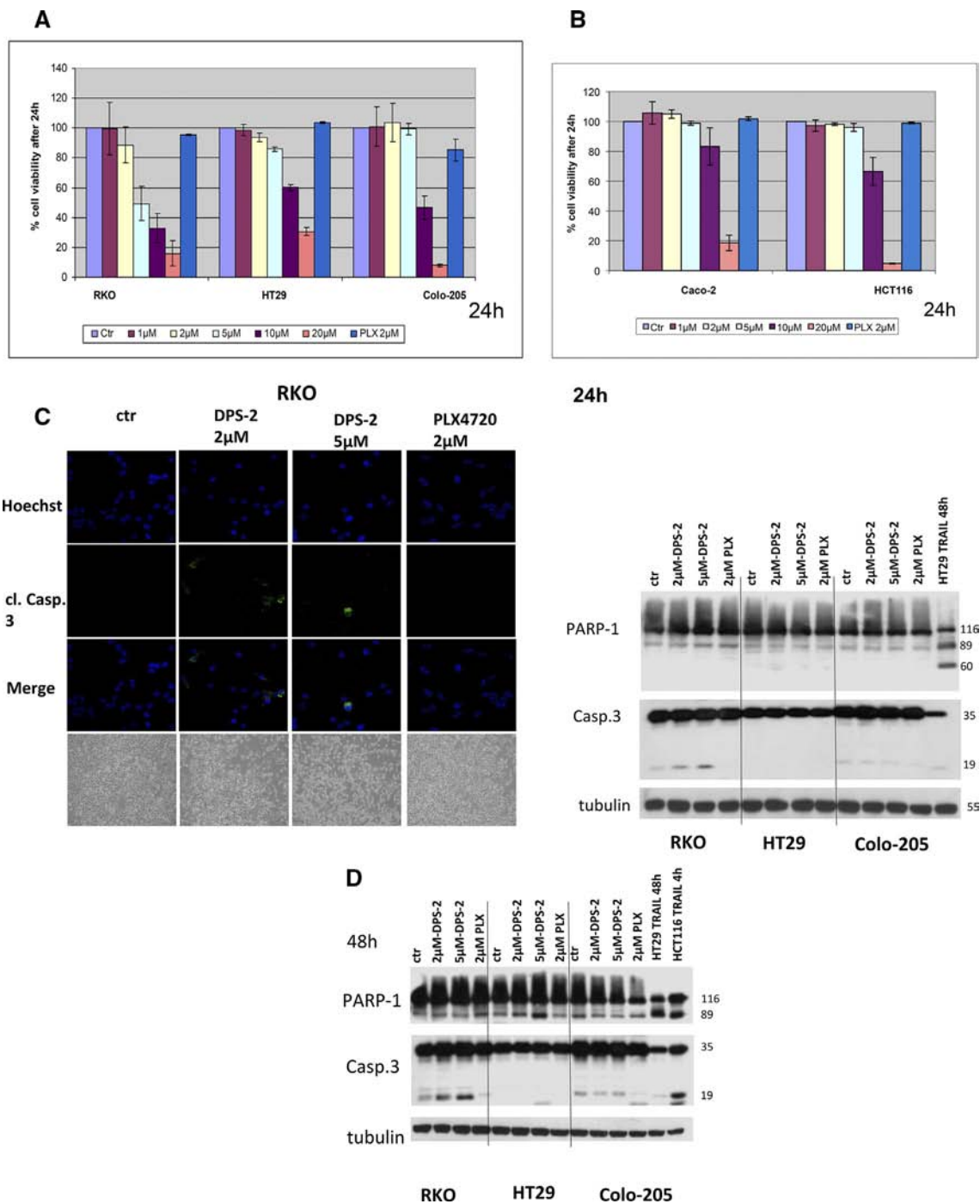
Figure 4. DPS-2 induces apoptosis and reduces autophagy in cancer cells lines.(A, B) Cell viability in RKO, HT29, Colo-205, Caco-2, HCT116, and DLD-1 cell lines were measured, using the SRB assay, after 24-hour treatment with increasing concentrations of DPS-2 inhibitor. Data are representative for two independent experiments, each of which was performed in duplicates. SD was used for error bar generation. (C, left panel) Light and confocal microscope images of 2D culture in RKO cell line after treatment with $2\,\mu M$ and $5\,\mu M$ of DPS-2 for 24 hours. For apoptotic marker staining, cells were incubated and stained with Hoechst (first line) and with cleaved Caspase 3 antibody (second line) and merged (third column) in order to detect the presence of apoptotic cell death due to treatment (second, third row), as compared to untreated control (first row). Cells were also visualized under light microscope (fourth row). PLX4720 was used as a negative control for apoptosis. (Right panel) Western blot analysis of protein levels of the apoptotic markers PARP-1 and Caspase-3 after 24-hour treatment with $2\,\mu M$ and $5\,\mu M$ of DPS-2 in RKO, HT29, and Colo-205 cell lines. Protein levels were normalized against tubulin. TRAIL was used as a positive control for the presence of apoptotic cell death. PLX4720 was used as a negative control for apoptosis. Data are representative for three independent experiments. (D) Western blot analysis of protein levels of the apoptotic markers PARP-1 and Caspase-3 after 48-hour treatment with $2\,\mu M$ and of DPS-2 in RKO, HT29, and Colo-205 cell lines. Protein levels were normalized against tubulin. (E) Light and confocal microscope images of 2D culture in HT29 and Colo-205 cell lines after treatment with $2\,\mu M$ and $5\,\mu M$ of DPS-2 for 48 hours. For apoptotic marker staining, cells were incubated and stained with Hoechst (first line) and with cleaved Caspase 3 antibody (second line) and merged (third line) in order to detect the presence of apoptotic cell death due to treatment (second, thi3rd column), as compared to untreated control (first row). Cells were also visualized under light microscope (fourth column). PLX4720 was used as a negative control for apoptosis. (F) Western blot analysis of protein levels of the necroptotic markers RIP-1 (RIP) and RIP-3 (RIPK3) and the autophagic marker p62 after 24 hours (left panel) and 48 hours (right panel) of treatment with $2\,\mu M$ and $5\,\mu M$ of DPS-2 in RKO, HT29, and Colo-205 cell lines. Protein levels were normalized against actin.
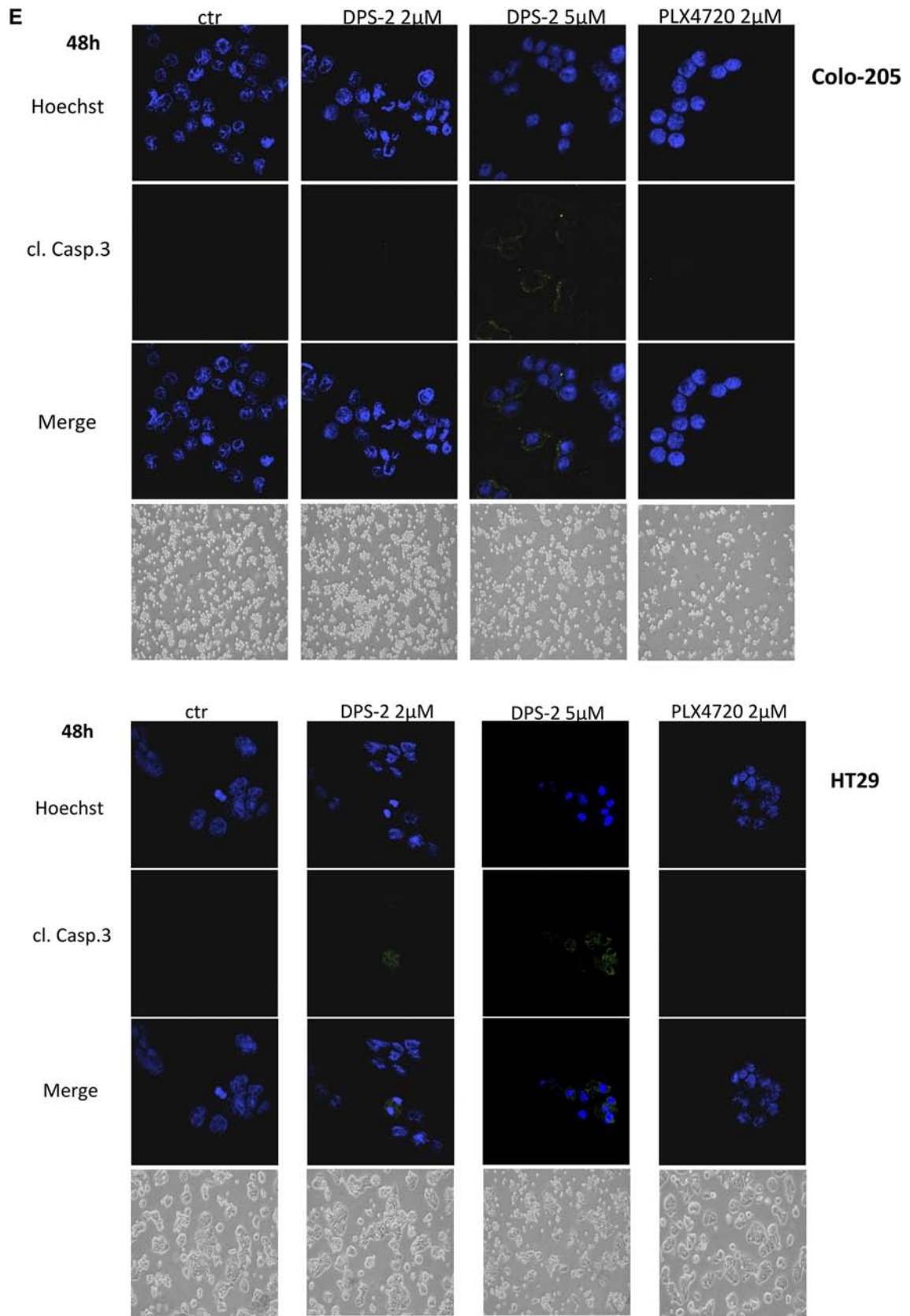
Figure 4. (*continued.*)
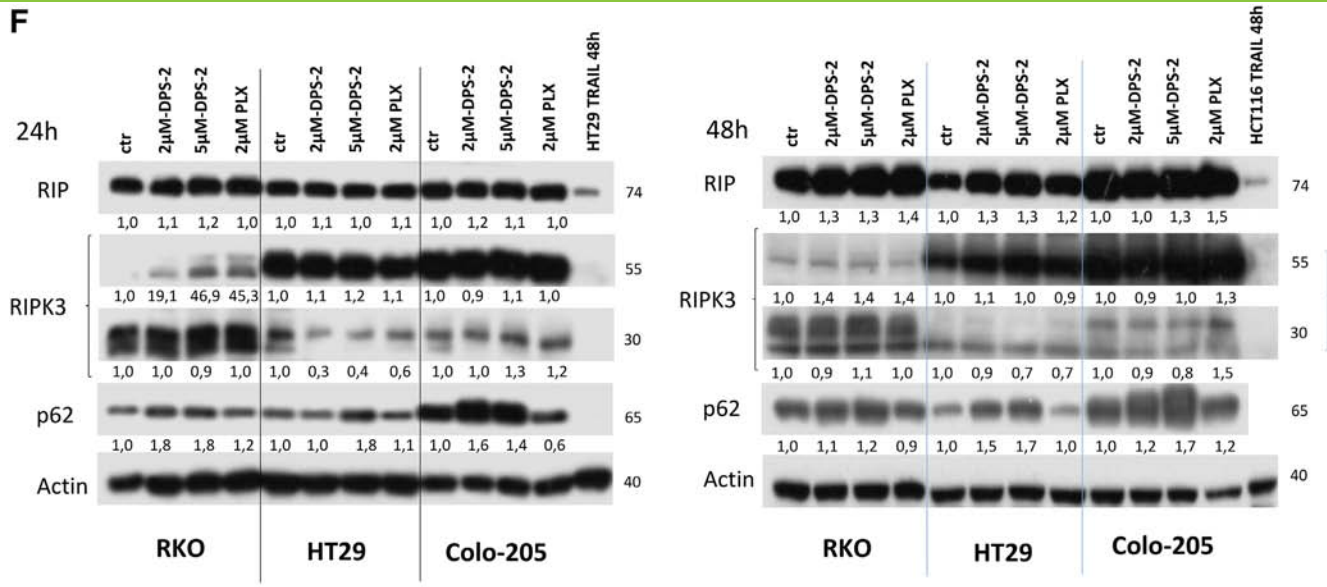
Figure 4. (*continued.*)

Effects of DPS-2 on apoptosis and autophagy in colon cancer cell lines

Since DPS-2 efficiently reduces cell viability in colon cancer cell lines after 72 hours of treatment, we then searched into its antiproliferative mechanism of action. First, we examined the effect of DPS-2 on cell viability after treatment for a shorter time period. Treatment with increasing concentrations of DPS-2 for 24 hours revealed a more modest efficiency of the compound in reducing cell viability of the examined cell lines RKO, HT29, Colo-205, Caco-2, and HCT116 as compared to its effect after 72-hour treatment. Except for RKO, cell viability in HT29, Colo-205, and HCT116 was reduced in DPS-2 concentrations equal to or higher than 10 μM (Figure 4, A and B). Caco-2 cell line was again more resistant, with its viability significantly reduced only after treatment with 20 μM of the compound (Figure 4B).

In order to examine thoroughly the cell viability effect of DPS-2 on colon cancer cell lines, analysis of apoptosis, as well as potential induction of either autophagy and/or necroptosis after cell treatments with DPS-2, was performed. Apoptotic marker staining of RKO cell line after 24-hour treatment with 2 μM or 5 μM DPS-2 revealed the presence of cleaved caspase-3 stained nuclei in both concentration treatments, as seen under confocal microscope (Figure 4C, left panel), revealing a putative induction of apoptosis by DPS-2, reflecting the reduction of cell viability even from the first 24 hours of treatment, observed in this cell line. The induction of apoptosis after these DPS-2 concentration treatments for 24 hours in RKO cells was also confirmed by the presence of Caspase-3 cleavage in Western blotting (Figure 4C, left panel). TRAIL treatment was used as a control for the induction of apoptosis in Western blots.

On the other hand, HT29 and Colo-205 cells did not show any evidence of apoptotic cell death either by cleaved Caspase-3 staining (data not shown) or by Caspase-3 cleavage detection using the Western blot assay after 24-hour treatment with 2 μM or 5 μM DPS-2 (Figure 4C, right panel). Interestingly, both cell lines HT29 and Colo-205 became sensitive to apoptotic cell death after a longer period of 48-hour treatment with DPS-2, as shown by Caspase-3 cleavage. In detail, 5 μM of DPS-2 caused Caspase-3 cleavage in HT29 cells, as shown both by staining with cleaved Caspase-3 antibody under confocal microscope and by the 17-kDa cleaved Caspase-3 detection in Western blot. Two micromolar DPS-

2 also resulted in cleaved Caspase-3 staining (Figure 4, D and E **HT29**). Treatment of Colo-205 with both 2 μM and 5 μM DPS-2 resulted in the 19-kDa cleaved Caspase-3 detection in Western blot, although the control sample of untreated cells also presented the same 19-kDa band of cleaved Caspase-3 (Figure 4D). However, staining with antibody for cleaved Caspase-3 under confocal microscope revealed a highly stained cell population after treatment with 5 μM DPS-2 (Figure 4E **Colo-205**).

Interestingly, autophagy- related p62 protein levels were induced in all cell lines RKO, HT29, and Colo-205 after treatment for both 24 hours and 48 hours with both 2 μM and 5 μM DPS-2 concentrations (Figure 4F), indicating a potent effect of DPS-2 on autophagy blockade.

Thus, the potent anticancer effect of DPS-2 can be the result of the activation of the apoptotic machinery in addition to the inhibition of autophagy, a tumor survival mechanism.

In turn, the potential effect of DPS-2 treatments on necroptosis was examined. Treatment of colon cancer cell lines RKO and HT29 with 2 μM and 5 μM of DPS-2 for 24 and 48 hours revealed a slight overexpression of RIP1 upon the longer time treatment. The same result was achieved in Colo-205 cells only after treatment with 5μM DPS-2 (Figure 4F). Moreover, RIPK3 isoform 1 (55 kDa) protein levels were in average not affected by the treatments, except for RKO, where an induction of this isoform 1 levels was recorded. On the other hand, RIPK3 isoform 2 (30 kDa) expression was strongly suppressed in HT29 cell line after treatment with both 2 μM and 5 μM DPS-2 after 24 and 48 hours, while the mildest reduction in these protein levels was observed in Colo-205 cells only after 48 hours of treatment. In RKO cells RIPK3 isoform 2, protein levels remained almost the same (Figure 4F).

Induction of apoptosis by DPS-2 in 3D colon cancer cultures

To test treatment conditions that mimic the real tumor microenvironment, Colo-205, one of the most sensitive to DPS-2 cell line, was grown in 3D cultures and formed tumors in Matrigel. Treatment with 2 μM or 5 μM DPS-2 was initiated after completion of tumor formation and lasted for 48 hours (Figure 5A) and 72 hours (Figure 5B). Though the tumor mass was not affected significantly due to the treatments, cell staining with Hoechst and cleaved
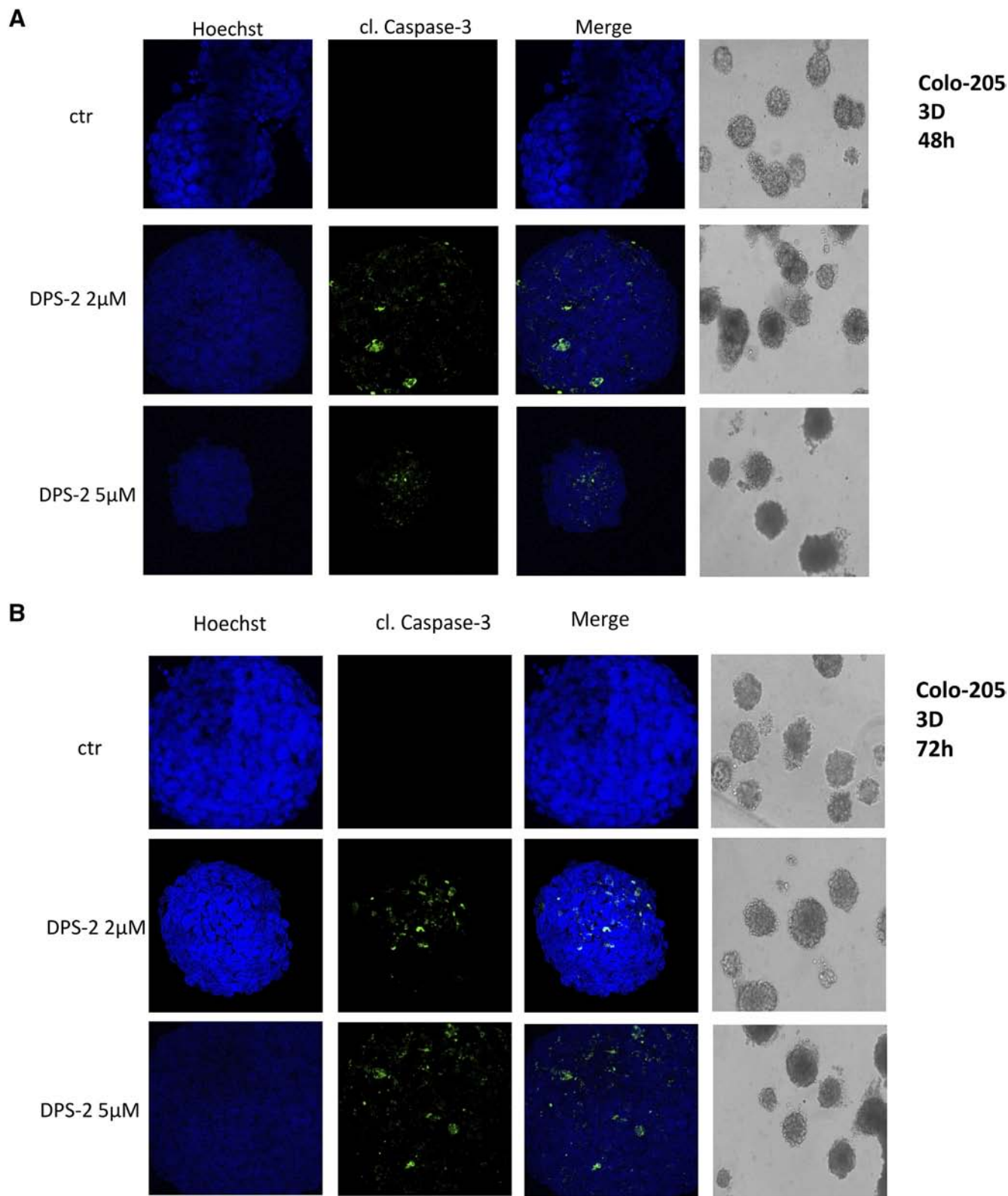
Figure 5. DPS-2 induces apoptosis of colon cancer cells in 3D cultures.Light and confocal microscope images of three-dimensional culture in Colo-205 cell line after treatment with 2 μM (second row) or 5 μM (third row) of DPS-2 for 48 hours (A) and 72 hours (B), as compared to control untreated tumors (first row). Tumor treatments started after 12e-day tumor formation. For apoptotic marker staining under confocal microscopy, Colo-205 tumors were incubated and stained with Hoechst (first column) and with cleaved Caspase 3 antibody (second column) and merged (third column) in order to detect the presence of apoptotic cell death, as compared to untreated control (first row). Tumors were also visualized under light microscope and their mass was measured (fourth column).

Caspase-3 under confocal microscopy revealed the presence of apoptotic cells within the tumors under all of the above treatments (Figure 5, *A* and *B*) Thus, it is obvious that the apoptotic effect of DPS-2 is also present in colon cancer tumors formed in 3D Matrigel.

DPS- 2 Acts as a Dual Inhibitor of MEK/ERK and PI3K/Akt Pathways

In order to determine molecular targets associated with colon cancer, which could be potent targets of DPS-2, we next examined the effect of DPS-2 treatments on molecular components of the different MAPK signaling pathways. Thus, we examined the effect of

$2 \mu M$ and $5 \mu M$ DPS-2 treatments on BRAF/MEK/ERK, PI3K/Akt/ mTOR, p-p38/ MAPK, and JNK/MAPK pathways. Treatments took place for 1 hour and 24 hours in order to assess the effect of the compound in both early and later time points. As a result, a potent inhibition of pERK1/2 was observed in Colo-205, which increased in higher concentration and longer time treatment, as shown by Western blot. PLX4720, a BRAFV600E selective inhibitor, was used as control for pMEK and pERK inhibition. In detail, pERK protein levels were reduced by 20% and 30% after treatment with $2 \mu M$ DPS-2 for 1 hour and 24 hours, respectively. The inhibition of ERK kinase phosphorylation was further increased, resulting in a 40% to
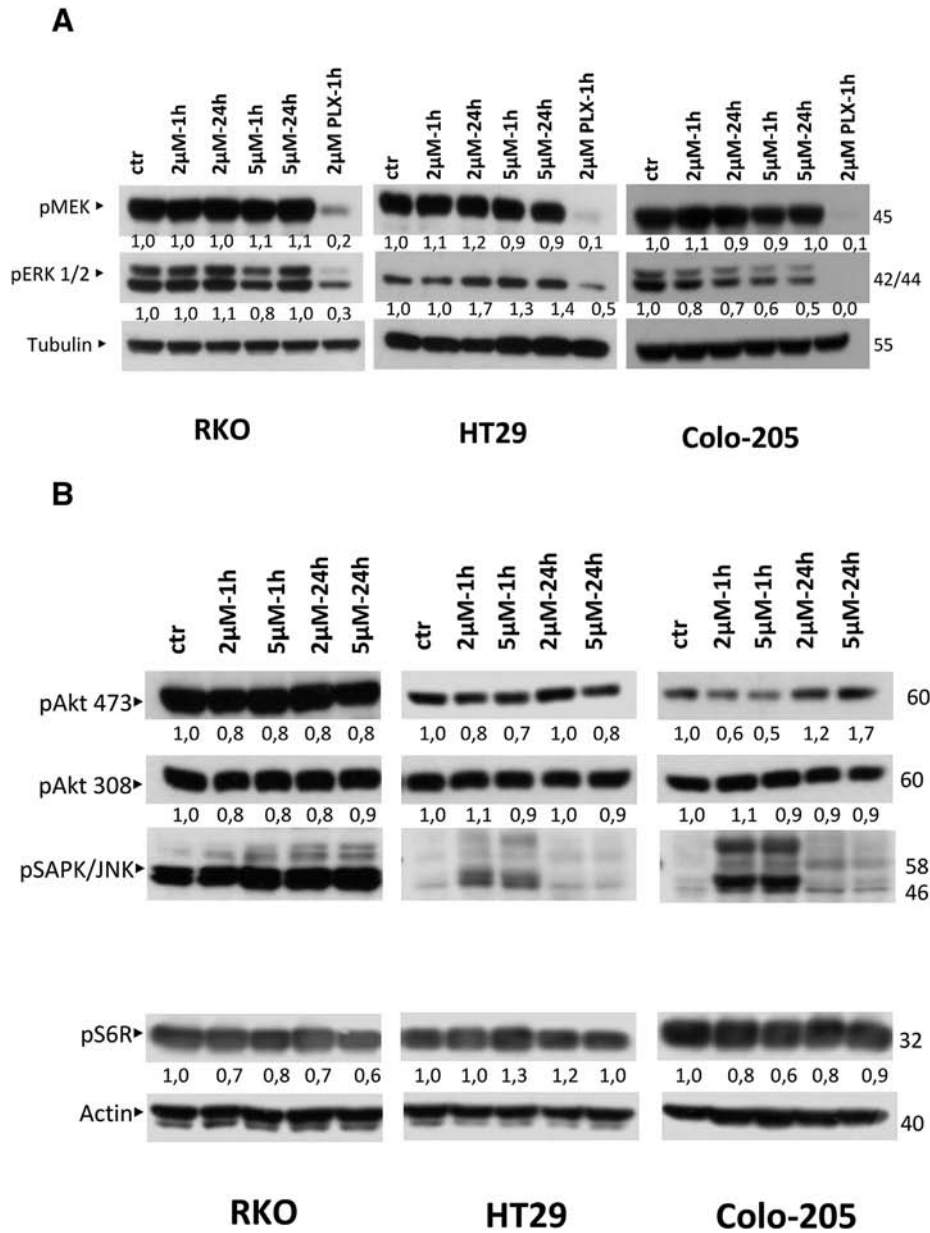
Figure 6. DPS-2 acts as a dual inhibitor of MEK/ERK and PI3K/AKT kinase pathways.(A) Western blot analysis of protein levels of p-MEK and p-ERK kinases after treatment with $2 \mu M$ and $5 \mu M$ of DPS-2 for 1 hour and 24 hours in RKO, HT29, and Colo-205 cell lines. PLX4720 was used as a positive control for MEK/ERK pathway inhibition. Protein levels were normalized against tubulin. (B) Western blot analysis of protein levels of p-Akt 473, p-Akt 308, p-SAPK/JNK, p-p38, and p-S6R after treatment with $2 \mu M$ and $5 \mu M$ of DPS-2 for 1 hour and 24 hours in RKO, HT29, and Colo-205 cell lines. Protein levels were normalized against actin. (C) Effect of DPS-2on phosphorylation in melanoma cell lines. The inhibition of pMEK, pERK, and pAKT by DPS-2 was examined in cell lines with BRAF V600E and NRAS Q61K mutations. Cell lines were treated with increasing concentrations of DPS-2 (0-10 μM) for 24 hours. The results are shown as % of activity in comparison with untreated controls (DMSO).
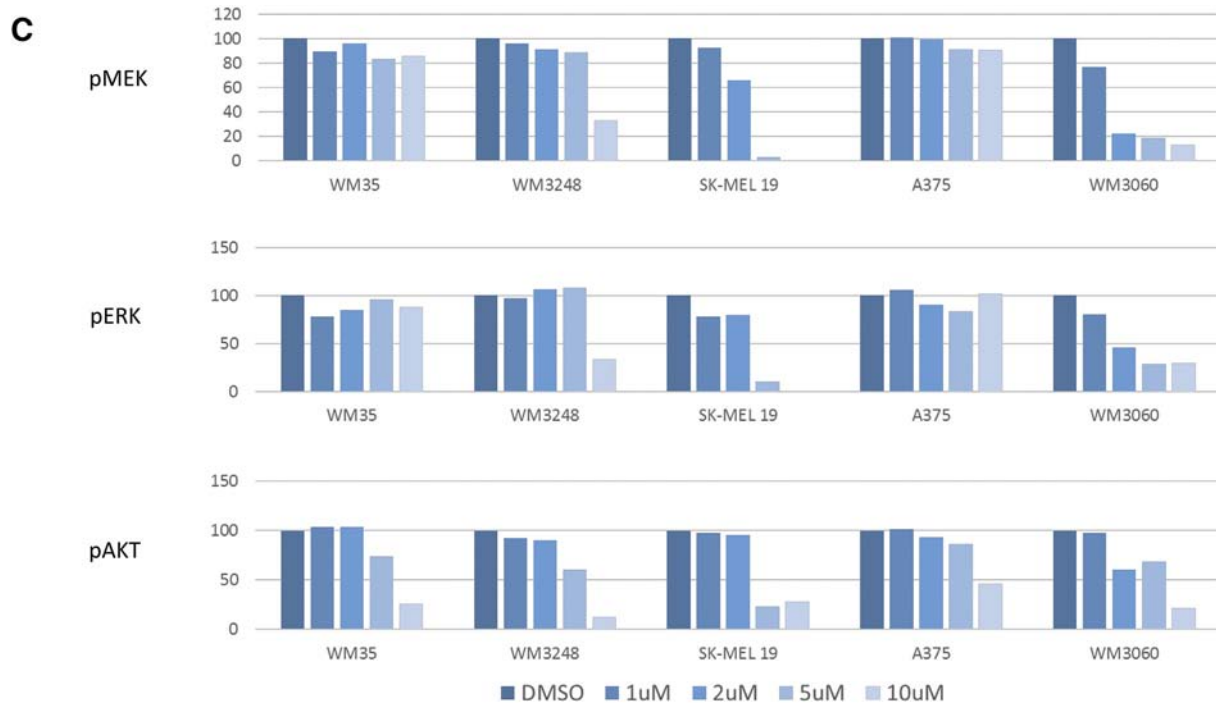
Figure 6. (*continued*.)

50% reduction on pERK levels after treatment with 5 µM DPS-2 for 1 hour and 24 hours, respectively (Figure 6*A*). In RKO cell line, pERK protein levels were reduced by 20% only after 1 hour early time treatment with 5 µM DPS-2. Interestingly, in HT29 cells, pERK levels were increased after treatments with the compound. pMEK protein levels were not significantly affected by DPS-2 treatments. These results strongly indicate a role for DPS-2 as a potent MEK pathway inhibitor, though in selected colon cancer cell lines.

Except for its action in the BRAF/MEK/ERK pathway, DPS-2 reduced pAkt 473 protein levels in RKO, HT29, and Colo-205 after 1-hour treatment in both concentrations 2 µM and 5 µM by 20%, 30% and 50%, respectively. The inhibitory effect was sustained after 24-hour treatments in RKO and HT29 but not in Colo-205 cells (Figure 6*B*). In RKO cells, DPS-2 reduced also pAkt 308 levels by 20%. In the same cell line, pS6R protein levels were reduced after both 1- and 24-hour treatment, with the inhibition reaching a level of 40% after 24-hour treatment with 5 µM DPS-2. Similarly, in the case of Colo-205, pS6R was suppressed after 1 hour of treatment with the highest concentration of DPS-2. In longer time treatments with the same concentration of the compound, as in 24 hours, pS6R levels are restored. In HT29 cells, there was no reduction in pS6R levels observed (Figure 6*B*). According to these data, DPS-2 can act as a potent inhibitor of Akt phosphorylation at position 473 and less at position 308. It may also modulate mTOR pathway in specific colon cancer cell lines.

Finally, treatment of RKO cells with 2 µM or 5 µM DPS-2 for both 1 hour and 24 hours resulted in an induction of pJNK, while the same was true for HT29 and Colo-205 only within the first hour of treatment. Furthermore, in Colo-205 cell line, the same concentration treatments resulted also in p-p38 induction after early time point treatments (data not shown). These findings indicate a possible role of the p-p38/ MAPK and JNK/MAPK pathways upon DPS-2 treatments, under some conditions in selected colon cancer cell lines.

In parallel analysis, the phosphoproteomic response to DPS-2 in melanoma cell lines was evaluated by measuring the activity of three major phosphoproteins (MEK1, ERK1, AKT1) involved in regulating melanoma growth and survival (Figure 6*C*). Activity of all three phosphoproteins was found significantly decreased in responsive cell lines (WM3248, SK-MEL19, and WM3060), with most responsive SK-MEL19 showing complete inhibition of MEK/ERK signaling in low micromolar concentrations. Interestingly, phosphorylation of MEK showed a vast decrease, especially in SK-MEL19 and WM3060, in contrast to CRC cell lines, where pMEK levels in Western blot analysis remained unaffected after treatment with the compound. DPS-2 administration also caused a decrease in phosphorylation of AKT in all five melanoma cell lines.

All the above data could indicate that the potent anticancer effect of DPS-2 can be associated to the dual inhibition of two key proliferative/survival pathways, like the MEK/ERK and PI3K/ Akt.

Inhibitory effects of DPS-2 on the development of colon tumors in vivo

Taking under consideration the antiproliferative, autophagy, and MEK/Akt kinase-suppressive roles of DPS-2 against colon cancer cell lines, our final goal was to examine whether DPS-2 could be also effective against colon tumors *in vivo*. Thus, nude mice were injected subcutaneously in both left and right flanks with Colo-205 colon cancer cells, and after tumor formation, mice were injected daily with 0.6 µg/µl diluted in 5% DMSO for a time period of 9 days after the initiation of the treatment. As shown in Figure 7, treatment with DPS-2 caused a reduction on tumor growth rate, resulting in tumor sizes of treated mice reduced by around seven times compared to untreated mice by the end of the injections. Statistical analysis of the results is presented in Tables 1 and 2. Thus, DPS-2 is very potent *in vivo* against mouse xenografts of colorectal tumor cells.
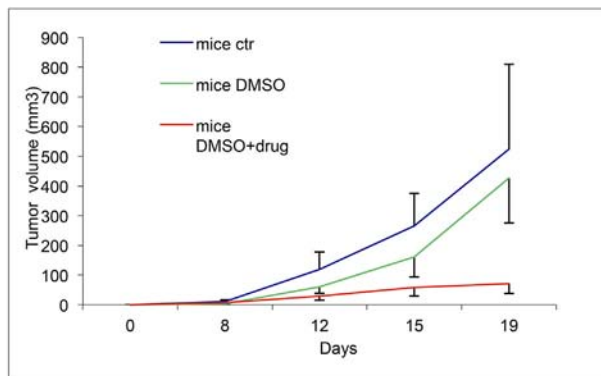
Mice	untreated	DMSO	DP-2 in DMSO
No. of sites injected	8	6	9
Onset of tumor formation (days)	8	8	8
Size of primary tumors at 8 days(mm³)	10,77±5,39	3,35±3,09	7,58±6,03
Size of primary tumors at 12 days(mm³)	118,75±58,62	59,47±20,57	28,46±13,28
Size of primary tumors at 15 days(mm³)	265,13±109,94	161,29±67,85	59,04±29,74
Size of primary tumors at 19 days(mm³)	523,94±285,32	426,08±150,73	71,21±32,83

Figure 7. DPS-2 blocks the development of Colo-205 tumors in nude mice.Inhibition of Colo-205 tumor development in nude mice after treatment with DPS-2. The mice were separated into three groups: untreated (mice ctr), DMSO treated (mice DMSO), and inhibitor treated (mice DMSO+drug). Chart lines represent tumor growth within a total period of 19 days after the injection of cancer cells. SD was used for error bar generation between all tumors of the same group of animals.

Discussion

Synthetic Approaches

Benzo[b]thiophene scaffold is one of the privileged structures in drug discovery as this core exhibits various biological activities allowing them to act as antimicrobial, anticancer, anti-inflammatory, antioxidant, antitubercular, antidiabetic, or anticonvulsant agents and many more. Further, numerous benzothiophene-based compounds as clinical drugs have been extensively used to treat various types of diseases with high therapeutic potency, which has led to their extensive developments [29].

Benzothiophene derivatives attracted considerable attention for medicinal chemists towards development of anticancer drugs, and several attempts were made for modifying the benzothiophene nucleus to improve their antitumor activities. Modifications on the benzothiophene nucleus have resulted in the synthesis of two anticancer drugs, namely, arzoxifene and raloxifene. Arzoxifene is a highly effective agent for prevention of mammary cancer induced in the rat by the carcinogen nitrosomethylurea and is significantly more potent than raloxifene in this regard [30]. Raloxifene is used in the prevention of osteoporosis in postmenopausal women and to reduce the risk of invasive breast cancer in postmenopausal women with osteoporosis and in postmenopausal women at high risk for invasive breast cancer [31]. Additionally, benzo[b]thiophen-3-yl)-2,2,2-tri-fluoroethanol interacts with the BPII pocket of BRAF, resulting in potent BRAF kinase inhibition [32].

Table 1. Statistical Analysis of the *In Vivo* Results According to Time Per Treatment Group

Time	Treatment Group	Time			
		Day 8	Day 12	Day 15	Day 19
Day 8	Control	ns	ns	ns	ns
	DMSO	ns	ns	ns	ns
	DPS-2	ns	ns	ns	ns
Day 12	Control	ns	ns	ns	ns
	DMSO	ns	ns	ns	ns
	DPS-2	ns	ns	ns	ns
Day 15	Control	***	**	ns	ns
	DMSO	**	ns	ns	ns
	DPS-2	ns	ns	ns	ns
Day 19	Control	***	***	***	ns
	DMSO	***	***	***	ns
	DPS-2	ns	ns	ns	ns

Analysis was performed using two-way ANOVA, repeated measures test.
ns: $P > .05$, * $P < .05$, ** $P < .01$, *** $P < .001$.

Table 2. Statistical Analysis of the *In Vivo* Results According to Treatment Group Per Time

Treatment Group	Time	Treatment Group		
		Control	DMSO	DPS-2
Control	Day 8	ns	ns	ns
	Day 12	ns	ns	ns
	Day 15	ns	ns	ns
	Day 19	ns	ns	ns
DMSO	Day 8	ns	ns	ns
	Day 12	ns	ns	ns
	Day 15	ns	ns	ns
	Day 19	ns	ns	ns
DPS-2	Day 8	ns	ns	ns
	Day 12	ns	ns	ns
	Day 15	***	ns	ns
	Day 19	***	***	ns

Analysis was performed using two-way ANOVA, repeated measures test.
ns: $p > .05$, * $p < .05$, ** $p < .01$, *** $p < .001$.

Encouraged by the above biological testing results, we proceeded to evaluate DPS-2 against CRC and melanoma tumor cells *in vitro* as well as colon tumors *in vivo*.

Necessity for treatment of KRAS- BRAF mutant CRC and RAS mutant melanoma. A new potent anticancer agent with apoptotic and autophagy- suppressing properties against CRC

Despite the recent development of efficient targeted therapies in oncology, so far, no specific cancer therapy against CRC tumors bearing KRAS or BRAF mutations has reached the clinic. Although there are already specific BRAF kinase inhibitors-targeted drugs in the metastatic BRAFV600E mutant melanoma with FDA approval (vemurafenib 2011, dabrafenib 2013), these inhibitors have not yielded positive results in clinical studies for patients with BRAF mutant colorectal cancer. Moreover, the inhibitors against BRAFV600E melanoma have opposite effects on tumors with normal BRAF and/or mutated RAS [33,34]. Novel drugs targeting either the KRAS/BRAF oncoproteins or their downstream components which mediate their oncogenic activities are currently being developed with the aim to revert KRAS/BRAF dependent tumor properties. Towards this direction, monotreatments of novel MEK inhibitors and their combinatorial treatments are in progress in different tumor types (reviewed by [35]). In the current study, synthesis and biological evaluation of a potent new anticancer agent DPS-2 against CRC and melanoma tumor cells are presented. DPS-2 can cause tumor cell apoptosis in 2D and 3D cultures, as well as in mouse xenografts. In tumors, autophagy can promote cancer cell survival and provide cancer cells with a highly plastic and dynamic mechanism to escape tumor therapies [36]. It is of interest that the potent anticancer effect of DPS-2 can be the result of the activation of the apoptotic machinery in addition to the inhibition of autophagy, a tumor survival mechanism. On the other hand, the activity of DPS-2 does not appear to be mediated by necroptotic mechanisms in most treatment protocols presented here.

Combinatorial and Dual BRAF/MEK/PI3K Inhibition for Cancer Therapy

Rational approaches for combination therapy strategies targeting the MAP kinase pathway are described in a recent review [37]. Resistance mechanisms to targeted therapeutic agents against BRAF/ MEK by reverse-translational approaches have recently facilitated the establishment of novel efficient combinatorial treatments of BRAF and MEK inhibitors against mutBRAF tumors, either in metastatic melanoma [38] or in non–small cell lung cancer [39]. As an alternative approach, RO5126766 is a first-in-class selective dual BRAF/CRAF and MEK inhibitor currently in early development for advanced solid tumors [40]. In the present study, evidence is presented that DPS-2 is a novel dual MEK/ERK and PI3K/AKT cell signaling pathway inhibitor in melanoma and colorectal cancer cells. Since these two pathways are key pathways for the proliferation and survival of tumor cells, the potent anticancer activity of the new inhibitor DPS-2 can be mediated at least partially through this dual inhibition.

It has been shown in several studies that PI3K pathway activation mediates resistance to MEK inhibitors [41]. Tumors with both KRAS and phosphoinositide 3-kinase mutations are unlikely to respond to the inhibition of the MEK pathway alone or the PI3K pathway alone but will require effective inhibition of both MEK and PI3K/AKT pathway signaling. Preclinical data suggest that BRAF/MEK and PI3K/mTOR inhibition may delay tumor growth but may not affect tumor size regression and is likely to be inferior to MEK and PI3K inhibition. The combination of specific PI3K inhibitors, rather than dual mTOR/PI3K inhibitors, with MEK inhibitors may result in greater synergy [42]. Clinical trials on dual targeted inhibition with MEK revealed that CRC patients harboring mutations in both pathways had tumor regression ranging between 2% and 64% when treated with PI3K and MAPK inhibitors. Dual pathway inhibition may potentially exhibit greater efficacy than single targeted therapy at the expense of greater toxicity [43].

In the present study, the potent anticancer effect of the new compound DPS-2 in 2D and 3D tumor cell cultures and in mouse xenografts is associated with efficient inhibition of MER/ERK and PI3K/AKT pathways known to be involved in colon cancer and melanoma progression. It is expected that DPS-2 potent activity can lead to further exploitation into new potential efficient anticancer treatments either alone or in combination, once further validated at the preclinical level and finally in the clinic.

Benefits of One Small Molecule Instead of Two or More for Blocking Two Pathways

Drug toxicity and low organism tolerability are two of the main drawbacks in drug-mediated cancer treatment. Thus, combinatorial treatments of solid tumors with small molecule inhibitors that target more than one crucial pathway, though effective, can lead to severe adverse effects [44,45]. On the other hand, the use of multitarget small molecule inhibitors, although appealing for bypassing acquired resistance of specific tumors to drug treatment, has shown dismal performances in clinical trials since these inhibitors usually demonstrate off-target toxicity due to their disability to distinguish between cancer and normal cells [46]. A solution to this problem would be the development of small molecule inhibitors with a narrower field of action and higher specificity. These could act on key kinases of the same [40,47] or cross-talking [48] pathways.

In the present study, we showed that DPS-2 is a single agent that acts as a dual MEK/ERK and PI3K/AKT pathway inhibitor, showing high efficiency in blocking ERK and AKT phosphorylation, respectively, in selected colon cancer and melanoma cell lines, as shown by decreased pERK and pAKT levels in Western blot analysis. Nevertheless, it is shown here that DPS-2 may have differential effects not only on CRC and melanoma cells but even on different cell lines of the same cancer type, an observation that has already been presented for other known inhibitors [49]. Interestingly, HT29 cell line was found resistant to DPS-2 action regarding both BRAF/MEK/ERK and PI3K/Akt/mTOR pathways, with pERK and pS6R protein levels becoming elevated upon DPS-2 treatment. Induction of phosphorylation of these proteins could be due to several factors. As a speculation, HT-29 express high levels of EGFR [50], which have been indicated as a causal factor for the observed intrinsic resistance of colorectal cancer cell lines to BRAFV600E inhibitor treatment [12]. The presence of P449T heterozygous mutation in PI3KCA in HT29 could also play a role for the observed resistance. Colo-205, the most sensitive cell line to DPS-2 treatment, is PI3KCA wild-type. We have previously correlated activity of BRAF/MEK/ERK pathway with the autophagy state in CRC lines [49]. According to this, HT29 shows intrinsic increased levels of autophagic markers, a fact which could contribute to the induction of ERK phosphorylation upon DPS-2 treatment. Finally, an interaction between ERK and S6R proteins has been established previously [51], which could somehow portray the concomitant increase in both markers. Definitely, a more detailed

investigation should take place in order to shed light on the possible mechanisms that contribute to the observed resistance to DPS-2 action.

The Need for In Vitro Toxicity Screening of Candidate Therapeutic Molecules

Preclinical toxicity screening is a crucial test for the assessment of any novel candidate drug before its potent further evaluation in clinical trials. Given that laboratory animal testing requires millions of small animal sacrifices for the *in vivo* evaluation of thousands of chemicals yearly, thus creating a huge ethic, economic, and ecologic burden to the societies worldwide, *in vitro* drug screening has arisen as an economically and ecologically advantageous alternative to predict human toxicity in reliable and easier manner.

Based on the above, apart from its efficiency on suppressing the viability of colon cancer and melanoma cell lines, the cytotoxic effect of DPS-2 on other mammalian cell lines was also assessed. More specifically, we used two validated cell models, globally used for the assessment of *in vitro* cytotoxicity: NIH3T3, an immortalized murine embryonic fibroblast cell line, and HepG2, a human hepatocellular carcinoma cell line [52]. Specifically, NIH 3T3 cells are very similar to BALB/c 3T3 cells, which are proposed by ICCVAM as standard models for the prediction of acute *in vitro* cytotoxicity [28]. In addition, we examined the cytotoxic effect of DPS-2 on a mesenchymal stem cell line isolated from human umbilical cord, WJ-MSCs, in order to also assess its effect on nontransformed cells. Notably, the antiproliferative effect of DPS-2 was mitigated in HepG2 and NIH3T3, with only concentrations higher than 12.5 μM being able to cause a reduction in the viability of these cells. More interestingly, treatment with DPS-2 had no significant suppressive effect on cell viability of WJ-MSC even in high concentrations (up to 100 μM) of the agent.

Taken together, the above results clearly suggest that DPS-2 is a potent anticancer agent against colon cancer and melanoma cells while at the same time being noncytotoxic for normal cells.

Author contributions

L. A., V. Z., A. P., and D. P. designed the study. M. G., N. A., J. R., E. T., and I. C. performed experiments. V. Z., A. P., and D. P. wrote and edited the paper with input from the other authors.

Conflicts of Interest

The authors declare no conflict of interest.

References

[1] Colussi D, Brandi G, Bazzoli F, and Ricciardiello L (2013). Molecular pathways involved in colorectal cancer: implications for disease behavior and prevention. *Int J Mol Sci* **14**, 16365–16385. http://dx.doi.org/10.3390/ijms140816365.

[2] Walther A, Johnstone E, Swanton C, Midgley R, Tomlinson I, and Kerr D (2009). Genetic prognostic and predictive markers in colorectal cancer. *Nat Rev Cancer* **9**, 489–499. http://dx.doi.org/10.1038/nrc2645.

[3] Thorstensen L, Lind GE, Lovig T, Diep CB, Meling GI, Rognum TOLothe RA (2005). Genetic and epigenetic changes of components affecting the WNT pathway in colorectal carcinomas stratified by microsatellite instability. *Neoplasia* **7**, 99–108. http://dx.doi.org/10.1593/neo.04448.

[4] Tripathi S, Belkacemi L, Cheung MS, and Bose RN (2016). Correlation between gene variants, signaling pathways, and efficacy of chemotherapy drugs against colon cancers. *Cancer Informat* **15**, 1–13. http://dx.doi.org/10.4137/CIN.S34506.

[5] Montagut C and Settleman J (2009). Targeting the RAF-MEK-ERK pathway in cancer therapy. *Cancer Lett* **283**, 125–134. http://dx.doi.org/10.1016/j.canlet.2009.01.022.

[6] Hoshino R, Chatani Y, Yamori T, Tsuruo T, Oka H, Yoshida O, Shimada Y, Ari-i S, Wada H, and Fujimoto J, et al (1999). Constitutive activation of the 41 –/43-kDa mitogen-activated protein kinase signaling pathway in human tumors. *Oncogene* **18**, 813–822. http://dx.doi.org/10.1038/sj.onc.1202367.

[7] Davies H, Bignell GR, Cox C, Stephens P, Edkins S, Clegg S, Teague J, Woffendin H, Garnett MJ, and Bottomley W, et al (2002). Mutations of the BRAF gene in human cancer. *Nature* **417**, 949–954. http://dx.doi.org/10.1038/nature00766.

[8] Tsai J, Lee JT, Wang W, Zhang J, Cho H, Mamo S, Bremer R, Gillette S, Kong J, and Haass NK, et al (2008). Discovery of a selective inhibitor of oncogenic B-Raf kinase with potent antimelanoma activity. *Proc Natl Acad Sci U S A* **105**, 3041–3046. http://dx.doi.org/10.1073/pnas.0711741105.

[9] Bollag G, Hirth P, Tsai J, Zhang J, Ibrahim PN, Cho H, Spevak W, Zhang C, Zhang Y, and Habets G, et al (2010). Clinical efficacy of a RAF inhibitor needs broad target blockade in BRAF-mutant melanoma. *Nature* **467**, 596–599. http://dx.doi.org/10.1038/nature09454.

[10] Chapman PB, Hauschild A, Robert C, Haanen JB, Ascierto P, Larkin J, Dummer R, Garbe C, Testori A, and Maio M, et al (2011). Improved survival with vemurafenib in melanoma with BRAF V600E mutation. *N Engl J Med* **364**, 2507–2516. http://dx.doi.org/10.1056/NEJMoa1103782.

[11] Yang H, Higgins B, Kolinsky K, Packman K, Bradley WD, Lee RJ, Schostack K, Simcox ME, Kopetz S, and Heimbrook D, et al (2012). Antitumor activity of BRAF inhibitor vemurafenib in preclinical models of BRAF-mutant colorectal cancer. *Cancer Res* **72**, 779–789. http://dx.doi.org/10.1158/0008-5472.CAN-11-2941.

[12] Prahallad A, Sun C, Huang S, Di Nicolantonio F, Salazar R, Zecchin D, Beijersbergen RL, Bardelli A, and Bernards R (2012). Unresponsiveness of colon cancer to BRAF(V600E) inhibition through feedback activation of EGFR. *Nature* **483**, 100–103. http://dx.doi.org/10.1038/nature10868.

[13] Kopetz S, Desai J, Chan E, Hecht JR, O'Dwyer PJ, Lee RJ, Nolop B, and Saltz L (2010). PLX4032 in metastatic colorectal cancer patients with mutant BRAF tumors. *J Clin Oncol* **28**, 3534. http://dx.doi.org/10.1200/jco.2010.28.15_suppl.3534.

[14] Tabernero J, Chan E, Baselga J, Blay JY, Chau I, Hyman DM, Raje NS, Wolf J, Sirzen F, and Veronese ML, et al (2014). VE-BASKET, a Simon 2-stage adaptive design, phase II, histology-independent study in nonmelanoma solid tumors harboring BRAF V600 mutations (V600m): Activity of vemurafenib (VEM) with or without cetuximab (CTX) in colorectal cancer (CRC). *J Clin Oncol* **32**, 3518. http://dx.doi.org/10.1200/jco.2014.32.15_suppl.3518.

[15] Yaeger R, Cercek A, O'Reilly EM, Reidy DL, Kemeny N, Wolinsky T, Capanu M, Gollub MJ, Rosen N, and Berger MF, et al (2015). Pilot trial of combined BRAF and EGFR inhibition in BRAF-mutant metastatic colorectal cancer patients. *Clin Cancer Res* **21**, 1313–1320. http://dx.doi.org/10.1158/1078-0432.CCR-14-2779.

[16] Do K, Speranza G, Bishop R, Khin S, Rubinstein L, Kinders RJ, Datiles M, Eugeni M, Lam MH, and Doyle LA, et al (2015). Biomarker-driven phase 2 study of MK-2206 and selumetinib (AZD6244, ARRY-142886) in patients with colorectal cancer. *Investig New Drugs* **33**, 720–728. http://dx.doi.org/10.1007/s10637-015-0212-z.

[17] Zimmer L, Barlesi F, Martinez-Garcia M, Dieras V, Schellens JH, Spano JP, Middleton MR, Calvo E, Paz-Ares L, and Larkin J, et al (2014). Phase I expansion and pharmacodynamic study of the oral MEK inhibitor RO4987655 (CH4987655)

in selected patients with advanced cancer with RAS-RAF mutations. *Clin Cancer Res* **20**, 4251–4261. http://dx.doi.org/10.1158/1078-0432.CCR-14-0341.

[18] Hatzivassiliou G, Liu B, O'Brien C, Spoerke JM, Hoeflich KP, Haverty PM, Soriano R, Forrest WF, Heldens S, and Chen H, et al (2012). ERK inhibition overcomes acquired resistance to MEK inhibitors. *Mol Cancer Ther* **11**, 1143–1154. http://dx.doi.org/10.1158/1535-7163.MCT-11-1010.

[19] Corcoran RB, Atreya CE, Falchook GS, Kwak EL, Ryan DP, Bendell JC, Hamid O, Messersmith WA, Daud A, and Kurzrock R, et al (2015). Combined BRAF and MEK inhibition with dabrafenib and trametinib in BRAF V600-mutant colorectal cancer. *J Clin Oncol* **33**, 4023–4031. http://dx.doi.org/10.1200/JCO.2015.63.2471.

[20] Halilovic E, She QB, Ye Q, Pagliarini R, Sellers WR, Solit DB, and Rosen N (2010). PIK3CA mutation uncouples tumor growth and cyclin D1 regulation from MEK/ERK and mutant KRAS signaling. *Cancer Res* **70**, 6804–6814. http://dx.doi.org/10.1158/0008-5472.CAN-10-0409.

[21] Cohen MH, Gootenberg J, Keegan P, and Pazdur R (2007). FDA drug approval summary: bevacizumab plus FOLFOX4 as second-line treatment of colorectal cancer. *Oncologist* **12**, 356–361. http://dx.doi.org/10.1634/theoncologist.12-3-356.

[22] Tabernero J, Yoshino T, Cohn AL, Obermannova R, Bodoky G, Garcia-Carbonero R, Ciuleanu TE, Portnoy DC, Van Cutsem E, and Grothey A, et al (2015). Ramucirumab versus placebo in combination with second-line FOLFIRI in patients with metastatic colorectal carcinoma that progressed during or after first-line therapy with bevacizumab, oxaliplatin, and a fluoropyrimidine (RAISE): a randomised, double-blind, multicentre, phase 3 study. *Lancet Oncol* **16**, 499–508. http://dx.doi.org/10.1016/S1470-2045(15)70127-0.

[23] Price TJ, Peeters M, Kim TW, Li J, Cascinu S, Ruff P, Suresh AS, Thomas A, Tjulandin S, and Zhang K, et al (2014). Panitumumab versus cetuximab in patients with chemotherapy-refractory wild-type KRAS exon 2 metastatic colorectal cancer (ASPECCT): a randomised, multicentre, open-label, non-inferiority phase 3 study. *Lancet Oncol* **15**, 569–579. http://dx.doi.org/10.1016/S1470-2045(14)70118-4.

[24] Douillard JY, Siena S, Cassidy J, Tabernero J, Burkes R, Barugel M, Humblet Y, Bodoky G, Cunningham D, and Jassem J, et al (2010). Randomized, phase III trial of panitumumab with infusional fluorouracil, leucovorin, and oxaliplatin (FOLFOX4) versus FOLFOX4 alone as first-line treatment in patients with previously untreated metastatic colorectal cancer: the PRIME study. *J Clin Oncol* **28**, 4697–4705. http://dx.doi.org/10.1200/JCO.2009.27.4860.

[25] Christodoulou I, Kolisis FN, Papaevangeliou D, and Zoumpourlis V (2013). Comparative evaluation of human mesenchymal stem cells of fetal (Wharton's jelly) and adult (adipose tissue) origin during prolonged in vitro expansion: considerations for cytotherapy. *Stem Cells Int* **2013**246134. http://dx.doi.org/10.1155/2013/246134.

[26] Malich G, Markovic B, and Winder C (1997). The sensitivity and specificity of the MTS tetrazolium assay for detecting the in vitro cytotoxicity of 20 chemicals using human cell lines. *Toxicology* **124**, 179–192.

[27] Jones CD, Jevnikar MG, Pike AJ, Peters MK, Black LJ, Thompson AR, Falcone JF, and Clemens JA (1984). Antiestrogens. 2. Structure-activity studies in a series of 3-aroyl-2-arylbenzo[b]thiophene derivatives leading to [6-hydroxy-2-(4-hydroxyphenyl)benzo[b]thien-3-yl] [4-[2-(1-piperidinyl)ethoxy]-phenyl]methanone hydrochloride (LY156758), a remarkably effective estrogen antagonist with only minimal intrinsic estrogenicity. *J Med Chem* **27**, 1057–1066.

[28] Services NTPUSDoHaH (2006). ICCVAM Test Method Evaluation Report (TMER): In Vitro Cytotoxicity Test Methods for Estimating Starting Doses for Acute Oral Systemic Toxicity Testing. [NIH Publication No. 07–4519] https://ntpniehsnihgov/pubhealth/evalatm/test-method-evaluations/acute-systemic-tox/in-vitro-validation/tmer/indexhtml; 2006.

[29] Keri RS, Chand K, Budagumpi S, Balappa Somappa S, Patil SA, and Nagaraja BM (2017). An overview of benzo[b]thiophene-based medicinal chemistry. *Eur J Med Chem* **138**, 1002–1033. http://dx.doi.org/10.1016/j.ejmech.2017.07.038.

[30] Overk CR, Peng KW, Asghodom RT, Kastrati I, Lantvit DD, Qin Z, Frasor J, Bolton JL, and Thatcher GR (2007). Structure-activity relationships for a family of benzothiophene selective estrogen receptor modulators including raloxifene and arzoxifene. *ChemMedChem* **2**, 1520–1526. http://dx.doi.org/10.1002/cmdc.200700104.

[31] Wallace OB, Richardson TI, and Dodge JA (2003). Estrogen receptor modulators: relationships of ligand structure, receptor affinity and functional activity. *Curr Top Med Chem* **3**, 1663–1682.

[32] Niculescu-Duvaz D, Niculescu-Duvaz I, Suijkerbuijk BM, Menard D, Zambon A, Davies L, Pons JF, Whittaker S, Marais R, and Springer CJ (2013). Potent BRAF kinase inhibitors based on 2,4,5-trisubstituted imidazole with naphthyl and benzothiophene 4-substituents. *Bioorg Med Chem* **21**, 1284–1304. http://dx.doi.org/10.1016/j.bmc.2012.12.035.

[33] Hatzivassiliou G, Song K, Yen I, Brandhuber BJ, Anderson DJ, Alvarado R, Ludlam MJ, Stokoe D, Gloor SL, and Vigers G, et al (2010). RAF inhibitors prime wild-type RAF to activate the MAPK pathway and enhance growth. *Nature* **464**, 431–435. http://dx.doi.org/10.1038/nature08833.

[34] Halaban R, Zhang W, Bacchiocchi A, Cheng E, Parisi F, Ariyan S, Krauthammer M, McCusker JP, Kluger Y, and Sznol M (2010). PLX4032, a selective BRAF (V600E) kinase inhibitor, activates the ERK pathway and enhances cell migration and proliferation of BRAF melanoma cells. *Pigment Cell Melanoma Res* **23**, 190–200. http://dx.doi.org/10.1111/j.1755-148X.2010.00685.x.

[35] Templeton IE and Musib L (2015). MEK inhibitors beyond monotherapy: current and future development. *Curr Opin Pharmacol* **23**, 61–67. http://dx.doi.org/10.1016/j.coph.2015.05.012.

[36] Maes H, Rubio N, Garg AD, and Agostinis P (2013). Autophagy: shaping the tumor microenvironment and therapeutic response. *Trends Mol Med* **19**, 428–446. http://dx.doi.org/10.1016/j.molmed.2013.04.005.

[37] Tolcher AW, Peng W, and Calvo E (2018). Rational approaches for combination therapy strategies targeting the MAP kinase pathway in solid tumors. *Mol Cancer Ther* **17**, 3–16. http://dx.doi.org/10.1158/1535-7163.MCT-17-0349.

[38] Ascierto PA, GA McArthur, Dreno B, Atkinson V, Liszkay G, Di Giacomo AM, Mandala M, Demidov L, Stroyakovskiy D, and Thomas L, et al (2016). Cobimetinib combined with vemurafenib in advanced BRAF(V600)-mutant melanoma (coBRIM): updated efficacy results from a randomised, double-blind, phase 3 trial. *Lancet Oncol* **17**, 1248–1260. http://dx.doi.org/10.1016/S1470-2045(16)30122-X.

[39] Planchard D, Smit EF, Groen HJM, Mazieres J, Besse B, Helland A, Giannone V, D'Amelio Jr AM, Zhang P, and Mookerjee B, et al (2017). Dabrafenib plus trametinib in patients with previously untreated BRAF(V600E)-mutant metastatic non-small-cell lung cancer: an open-label, phase 2 trial. *Lancet Oncol* **18**, 1307–1316. http://dx.doi.org/10.1016/S1470-2045(17)30679-4.

[40] Martinez-Garcia M, Banerji U, Albanell J, Bahleda R, Dolly S, Kraeber-Bodere F, Rojo F, Routier E, Guarin E, and Xu ZX, et al (2012). First-in-human, phase I dose-escalation study of the safety, pharmacokinetics, and pharmacodynamics of RO5126766, a first-in-class dual MEK/RAF inhibitor in patients with solid tumors. *Clin Cancer Res* **18**, 4806–4819. http://dx.doi.org/10.1158/1078-0432.CCR-12-0742.

[41] Wee S, Jagani Z, Xiang KX, Loo A, Dorsch M, Yao YM, Sellers WR, Lengauer C, and Stegmeier F (2009). PI3K pathway activation mediates resistance to MEK inhibitors in KRAS mutant cancers. *Cancer Res* **69**, 4286–4293. http://dx.doi.org/10.1158/0008-5472.CAN-08-4765.

[42] Temraz S, Mukherji D, and Shamseddine A (2015). Dual inhibition of MEK and PI3K pathway in KRAS and BRAF mutated colorectal cancers. *Int J Mol Sci* **16**, 22976–22988. http://dx.doi.org/10.3390/ijms160922976.

[43] Shimizu T, Tolcher AW, Papadopoulos KP, Beeram M, Rasco DW, Smith LS, Gunn S, Smetzer L, Mays TA, and Kaiser B, et al (2012). The clinical effect of the dual-targeting strategy involving PI3K/AKT/mTOR and RAS/MEK/ERK pathways in patients with advanced cancer. *Clin Cancer Res* **18**, 2316–2325. http://dx.doi.org/10.1158/1078-0432.CCR-11-2381.

[44] Algazi AP, Posch C, Ortiz-Urda S, Cockerill A, Munster PN, and Daud A (2014). A phase I trial of BKM120 combined with vemurafenib in BRAFV600E/K mutant advanced melanoma. *J Clin Oncol* . http://dx.doi.org/10.1200/jco.2014.32.15_suppl.9101.

[45] Tabernero J, Van Geel R, Guren TK, Yaeger RD, Spreafico A, Faris JE, Yoshino T, Yamada Y, Kim TW, and Bendell JC, et al (2016). Phase 2 results: encorafenib (ENCO) and cetuximab (CETUX) with or without alpelisib (ALP) in patients with advanced BRAF-mutant colorectal cancer (BRAFm CRC). *J Clin Oncol* **34**. http://dx.doi.org/10.1200/JCO.2016.34.15_suppl.3544.

[46] Cheng H and Force T (2010). Why do kinase inhibitors cause cardiotoxicity and what can be done about it? *Prog Cardiovasc Dis* **53**, 114–120. http://dx.doi.org/10.1016/j.pcad.2010.06.006.

[47] Liu TJ, Koul D, LaFortune T, Tiao N, Shen RJ, Maira SM, Garcia-Echevrria C, and Yung WK (2009). NVP-BEZ235, a novel dual phosphatidylinositol 3-kinase/mammalian target of rapamycin inhibitor, elicits multifaceted antitumor activities in human gliomas. *Mol Cancer Ther* **8**, 2204–2210. http://dx.doi.org/10.1158/1535-7163.MCT-09-0160.

[48] Yu P, Ye L, Wang H, Du G, Zhang J, Zhang J, and Tian J (2015). NSK-01105 inhibits proliferation and induces apoptosis of prostate cancer cells by blocking the Raf/MEK/ERK and PI3K/Akt/mTOR signal pathways. *Tumour Biol* **36**, 2143–2153. http://dx.doi.org/10.1007/s13277-014-2824-x.

[49] Goulielmaki M, Koustas E, Moysidou E, Vlassi M, Sasazuki T, Shirasawa S, Zografos G, Oikonomou E, and Pintzas A (2016). BRAF associated autophagy exploitation: BRAF and autophagy inhibitors synergise to efficiently overcome resistance of BRAF mutant colorectal cancer cells. *Oncotarget* **7**, 9188–9221. http://dx.doi.org/10.18632/oncotarget.6942.

[50] Solmi R, Lauriola M, Francesconi M, Martini D, Voltattorni M, Ceccarelli C, Ugolini G, Rosati G, Zanotti S, and Montroni I, et al (2008). Displayed correlation between gene expression profiles and submicroscopic alterations in response to cetuximab, gefitinib and EGF in human colon cancer cell lines. *BMC Cancer* **8**227. http://dx.doi.org/10.1186/1471-2407-8-227.

[51] Roux PP, Shahbazian D, Vu H, Holz MK, Cohen MS, Taunton J, Sonenberg N, and Blenis J (2007). RAS/ERK signaling promotes site-specific ribosomal protein S6 phosphorylation via RSK and stimulates cap-dependent translation. *J Biol Chem* **282**, 14056–14064. http://dx.doi.org/10.1074/jbc.M700906200.

[52] Shukla SJ, Huang R, Austin CP, and Xia M (2010). The future of toxicity testing: a focus on in vitro methods using a quantitative high-throughput screening platform. *Drug Discov Today* **15**, 997–1007. http://dx.doi.org/10.1016/j.drudis.2010.07.007.